



UNIVERSIDADE ESTADUAL DE CAMPINAS
SISTEMA DE BIBLIOTECAS DA UNICAMP
REPOSITÓRIO DA PRODUÇÃO CIENTIFICA E INTELECTUAL DA UNICAMP

Versão do arquivo anexado / Version of attached file:

Versão do Editor / Published Version

Mais informações no site da editora / Further information on publisher's website:

<https://www.sciencedirect.com/science/article/pii/S0370269324006245>

DOI: 10.1016/j.physletb.2024.139066

Direitos autorais / Publisher's copyright statement:

©2025 by Elsevier. All rights reserved.

DIRETORIA DE TRATAMENTO DA INFORMAÇÃO

Cidade Universitária Zeferino Vaz Barão Geraldo
CEP 13083-970 – Campinas SP
Fone: (19) 3521-6493
<http://www.repositorio.unicamp.br>



Letter

Measurement of ${}^3_{\Lambda}\text{H}$ production in Pb–Pb collisions at $\sqrt{s_{\text{NN}}} = 5.02 \text{ TeV}$

ALICE Collaboration *



ARTICLE INFO

Editor: M. Doser

Dataset link: <https://www.hepdata.net/record/ins2791616>

ABSTRACT

The first measurement of ${}^3_{\Lambda}\text{H}$ and ${}^3_{\bar{\Lambda}}\text{H}$ differential production with respect to transverse momentum and centrality in Pb–Pb collisions at $\sqrt{s_{\text{NN}}} = 5.02 \text{ TeV}$ is presented. The ${}^3_{\Lambda}\text{H}$ has been reconstructed via its two-charged-body decay channel, i.e., ${}^3_{\Lambda}\text{H} \rightarrow {}^3\text{He} + \pi^-$. A Blast-Wave model fit of the p_T -differential spectra of all nuclear species measured by the ALICE collaboration suggests that the ${}^3_{\Lambda}\text{H}$ kinetic freeze-out surface is consistent with that of other nuclei. The ratio between the integrated yields of ${}^3_{\Lambda}\text{H}$ and ${}^3\text{He}$ is compared to predictions from the statistical hadronisation model and the coalescence model, with the latter being favoured by the presented measurements.

1. Introduction

Relativistic heavy-ion collisions provide a rich environment for the study of nuclei, hypernuclei, and their charge conjugates. Hypernuclei are nuclei that have at least one hyperon among their constituents. The additional strange baryon leads to a unique nuclear system that can help to benchmark the interactions among hyperons and nucleons. Understanding such interactions has become particularly relevant in recent years due to their important connections with the modelling of the equation-of-state of dense astrophysical objects, such as the neutron stars [1,2]. In fact, a precise knowledge of the two-body (Y–N) and three-body (Y–N–N) hyperon–nucleon forces allows for determining whether the presence of hyperons in the innermost core of neutron stars, which is known to be energetically favourable, reconciles with the recent observations of large-mass neutron stars [3,4]. Multiple studies analysing particle momentum correlations [5,6] play a direct role in establishing these interactions. In a complementary approach, the lifetime and the binding energy of a hypernucleus reflect the strength of the Y–N and Y–N–N forces [7–9].

The lightest known hypernucleus is the hypertriton (${}^3_{\Lambda}\text{H}$), composed of a proton, a neutron, and a Λ hyperon. As such, it represents the simplest system to study the interaction among Λ hyperons and nucleons. Early experiments studied ${}^3_{\Lambda}\text{H}$ using nuclear emulsions and helium bubble chambers [10–14]. These experiments obtained results with large statistical uncertainties. In recent years, more precise measurements have been performed by ALICE [15–18] and STAR [19–23]. Collaborations in relativistic heavy-ion collisions at the CERN LHC and BNL RHIC colliders. Such measurements contributed in determining that the ${}^3_{\Lambda}\text{H}$ is a loosely bound state with a Λ separation energy, B_{Λ} , of the order of one hundred keV, and has an average lifetime very close to the free Λ one [24]. With such properties, the hypertriton wave function

is expected to have a radial extension of approximately 5 fm [25–27], considerably larger than the other nuclei with a mass number equal to three and comparable in size to the fireball created in Pb–Pb collisions.

There are two main classes of models used to explain the formation of nuclei in Pb–Pb collisions: the statistical hadronisation model (SHM) and the coalescence model. While the SHM is insensitive to the structure of the particle being produced [28–32], the coalescence model relies on the knowledge of the particle wave function to produce predictions [33–39]. There is a wealth of variations for each class of models but based on similar approach. In the SHM, the production cross section of a specific particle is determined solely by a temperature, denoted as chemical freeze-out temperature, the volume of the system created in the collision, the quantum numbers, and the mass of the particle. In Pb–Pb collisions, the grand canonical formulation of the SHM has proven to be very successful in describing the yields of light flavoured hadrons [28]. Based on the two parameters from the analysis of light hadrons, the SHM then provides a parameter-free prediction of the yields of (hyper)nuclei. In the coalescence model, the production rate of nuclei is given by the convolution between the phase space of the nucleons produced in the collision and the nuclear wave function, according to the Wigner function formalism [40]. These two models give similar predictions for the yield ratios of most ordinary nuclei (e.g. d/p) [35–37] and qualitatively describe the available experimental data at the LHC [41–52]. However, when it comes to a tight configuration or a loosely-bound state, the prediction of the SHM and the coalescence model for particle ratios diverge significantly in all collision systems. For example, recent studies on the yield of ${}^4\text{He}$ in Pb–Pb collisions show an agreement with the SHM while the coalescence model failed to explain it [52]. Conversely, the ${}^3_{\Lambda}\text{H}/\Lambda$ ratio in p–Pb collisions [17] is only well-described by the coalescence predictions. This discrepancy indicates that the nucleosynthesis mech-

* E-mail address: alice-publications@cern.ch.

anism [53,54] still needs further investigation with new experimental measurements.

This letter presents the first measurement of the ${}^3\Lambda\text{H}$ production in Pb–Pb collisions at a center-of-mass energy per nucleon pair $\sqrt{s_{\text{NN}}} = 5.02 \text{ TeV}$. In Sec. 2 the ALICE apparatus and the analysis method are described, whereas the results are discussed in Sec. 3.

2. The ALICE detector and analysis details

The ALICE apparatus is composed of several specialised detectors, as detailed in [55]. In this analysis, ${}^3\Lambda\text{H}$ are reconstructed using both the Inner Tracking System (ITS) [56] and the Time Projection Chamber (TPC) [57] detectors. The ITS is the closest central-barrel detector to the beam pipe and comprises six cylindrical layers. The primary role of ITS is to reconstruct charged-particle trajectories and to measure precisely the position of the interaction vertices. The TPC is a gaseous detector employed as the primary tracking and particle identification (PID) device in ALICE. The TPC is used to identify charged particles by measuring their specific energy loss. Both ITS and TPC are placed in a homogeneous magnetic field of 0.5 T produced by a solenoidal magnet. These two detectors cover the entire azimuth in the pseudorapidity range $|\eta| < 0.9$. The centrality determination and trigger are provided by a pair of forward ($2.8 < \eta < 5.1$) and backward ($-3.7 < \eta < -1.7$) detectors called VOA and VOC [58], respectively. The coincidence of a signal in the VOA and a signal in the VOC is used as a minimum-bias trigger. Additionally, two thresholds on the minimum amount of charge deposited on the VO detector are implemented to trigger online on central and semi-central Pb–Pb collisions. These thresholds are defined by the Glauber model fit to the VO detector signal amplitudes [58,59].

The data sample employed in this analysis has been collected during the LHC 2018 Pb–Pb run at $\sqrt{s_{\text{NN}}} = 5.02 \text{ TeV}$. Based on the signal amplitudes of the VO detectors, three centrality classes are considered (from central to peripheral collisions): 0–10%, 10–30%, and 30–50%. The centrality classes are labelled according to the corresponding percentiles of the Pb–Pb hadronic interaction cross section. The stored events, categorized into the 0–10% and 30–50% classes, are enriched by the online trigger on central and semi-central collisions. In total, approximately 210 million events are studied. At the LHC energies, approximately the same number of ${}^3\Lambda\text{H}$ and ${}^3\bar{\Lambda}\text{H}$ are produced [60]. Therefore, the results of ${}^3\Lambda\text{H}$ and ${}^3\bar{\Lambda}\text{H}$ are averaged. In the following, we use the notation ${}^3\Lambda\text{H}$ for both particle and antiparticle.

A dedicated Monte Carlo (MC) simulated sample has been employed for optimising the ${}^3\Lambda\text{H}$ selection and evaluating the efficiency corrections. The MC sample consists of ${}^3\Lambda\text{H}$ signal injected on top of underlying Pb–Pb collisions, which are simulated with the HIJING event generator [61]. In each MC event, 80 ${}^3\Lambda\text{H}$ are injected. The transverse momentum (p_{T}) distribution of the injected signal is given by the Blast-Wave [62] function, with parameters taken from fit to the ${}^3\text{He}$ p_{T} spectra [51]. The particle transport through the detector material is done using GEANT4 [63], which simulates both the interaction with the material and the weak decay kinematics of the ${}^3\Lambda\text{H}$.

In this analysis, ${}^3\Lambda\text{H}$ candidates are reconstructed via the two-charged-body mesonic decay channel ${}^3\Lambda\text{H} \rightarrow {}^3\text{He} + \pi^-$ (and the related charge conjugated process). Firstly, a preselection method is performed. Tracks that have specific energy loss in the TPC compatible within 5σ to that of ${}^3\text{He}$ or π tracks are employed to reconstruct the ${}^3\Lambda\text{H}$ decay topology with the algorithm used in previous analyses [15–17]. The reconstruction of ${}^3\Lambda\text{H}$ candidates employed the ALICE secondary vertex finder method which pairs opposite-sign ${}^3\text{He}$ and π candidate tracks. The tracks are required to have more than 50 hits in TPC ($N_{\text{cls}}^{\text{TPC}}$) and good fit quality ($\chi^2/N_{\text{cls}}^{\text{TPC}} < 4$). In order to mitigate the contamination from ${}^3\text{He}$ produced in the interaction with materials, an additional selection $p_{\text{T}} > 1.2 \text{ GeV}/c$ is imposed for ${}^3\text{He}$. Additional selection criteria are used by combining data on the decay kinematics and the position of the

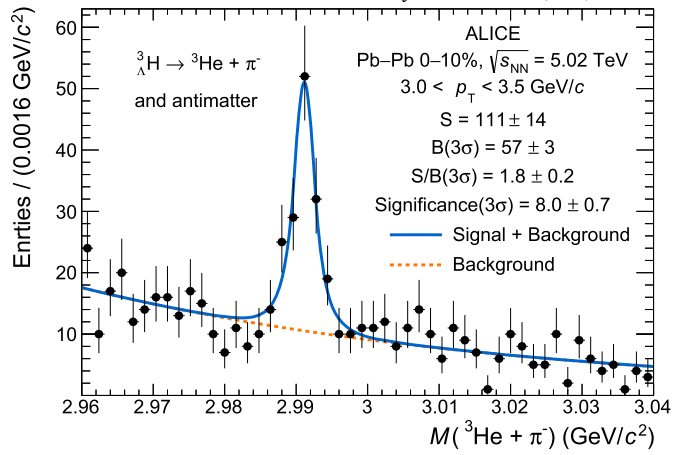


Fig. 1. Invariant-mass distribution of selected ${}^3\Lambda\text{H}$ candidates in the centrality class 0–10% and p_{T} interval $3 < p_{\text{T}} < 3.5 \text{ GeV}/c$ fitted with a function which is the sum of a double-sided Crystal Ball signal and an exponential background. Vertical lines represent the statistical uncertainties.

decay vertex. The selections include the maximum distance-of-closest-approach (DCA) of the decay products to the primary vertex ($\text{DCA}_{\text{toPV}} < 8 \text{ cm}$) and among the daughter tracks themselves ($\text{DCA}_{\text{tracks}} < 1.6 \text{ cm}$), and the cosine of the angle between the ${}^3\Lambda\text{H}$ momentum vector and the straight line connecting the primary and secondary vertices ($\cos \theta_{\text{P}}$). The selection on $\cos \theta_{\text{P}}$ is set as a function of the proper decay time of the candidates such to ensure a 95% efficiency for reconstructing true ${}^3\Lambda\text{H}$.

The main selection step consists of combining the candidate features in a gradient-boosted decision tree classifier (BDT) [64,65] that is employed for the ${}^3\Lambda\text{H}$ signal selection. The BDT is a supervised learning algorithm that determines how to differentiate between two or more classes, specifically signal and background in this context, by analysing sets of examples referred to as the training sets. In this analysis, the training sets consist of ${}^3\Lambda\text{H}$ signal candidates obtained from the MC sample and background candidates from paired like-sign ${}^3\text{He}$ and π tracks from the data. For each ${}^3\Lambda\text{H}$ candidate, the BDT combines a set of topological and single-track variables to produce a score, which serves to separate signal and background. The variables do not exhibit correlation with the ${}^3\text{He}-\pi$ invariant mass and are: the decay length in the rest frame ct , the $\cos \theta_{\text{P}}$, the PID information for ${}^3\text{He}$, the DCA to the primary vertex for both ${}^3\text{He}$ and π tracks, the DCA between ${}^3\text{He}$ and π , and the number of clusters of the ${}^3\text{He}$ track in the TPC. Candidates with a BDT score exceeding a specified threshold are classified as signal. This threshold is determined to optimise the expected signal significance, taking into account the predicted production yield according to the SHM for the ${}^3\Lambda\text{H}$, as well as the background rate observed from like-sign ${}^3\text{He}$ and π pairs.

The BDT training and testing steps and the ${}^3\Lambda\text{H}$ yield computation have been performed in different centrality and p_{T} intervals independently. The ${}^3\Lambda\text{H}$ signal is extracted from the invariant-mass distribution after rejecting candidates whose score is lower than the BDT model threshold. An unbinned maximum-likelihood fit is performed to the ${}^3\Lambda\text{H}$ invariant-mass distribution, employing a double-sided Crystal Ball (DSCB) [66] function and an exponential function to model the signal and the background components of the spectrum, respectively. The parameters of the DSCB function are fixed using the MC sample leaving only the mean and the normalisation of the DSCB free. Fig. 1 shows an example of the invariant-mass fit in the most central collisions and in the p_{T} interval $3 < p_{\text{T}} < 3.5 \text{ GeV}/c$. The number of detected ${}^3\Lambda\text{H}$ is obtained from the integral of the DSCB function. However, this number has to be corrected to account for the detection efficiency, the branching ratio (B.R.), and the absorption of the ${}^3\Lambda\text{H}$ in the ALICE detector material. The detection efficiency comprises several components, including the acceptance of the ALICE detector, the absorption of daughter tracks, and the

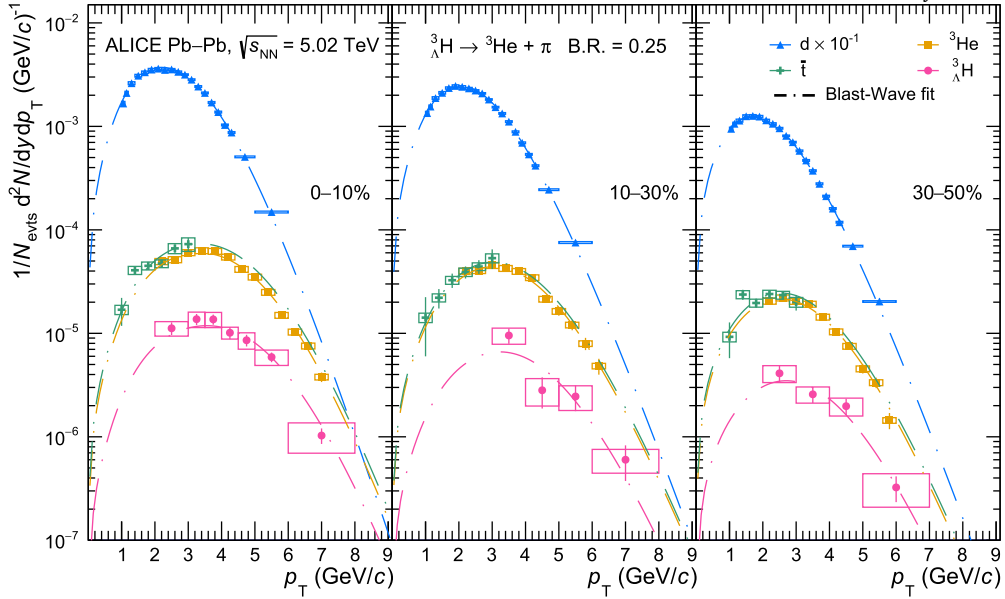


Fig. 2. Deuteron (d), antitriton (\bar{t}), ${}^3\text{He}$ [51], and ${}^3\text{H}$ spectra measured in Pb–Pb collisions at $\sqrt{s_{\text{NN}}} = 5.02 \text{ TeV}$. Each panel shows a centrality interval and different nuclei are reported with different colours. For ${}^3\text{H}$, the average spectra between particles and antiparticles is employed. The width of the boxes refers to the range of the p_{T} intervals, while their height represents the systematic uncertainties. The vertical lines are the statistical uncertainties. The combined Blast-Wave fit parameters for d , \bar{t} , ${}^3\text{He}$, and ${}^3\text{H}$ are listed in Table 1.

selection efficiency. It can be directly computed using the MC sample in different centrality and p_{T} intervals. The detection efficiency increases with the ${}^3\text{H}$ p_{T} and ranges from 10% to 38%. The branching ratio is set to 0.25 ± 0.023 according to Ref. [7]. Finally, the absorption correction (C_{abs}) is computed by simulating the interaction of ${}^3\text{H}$ with the ALICE detector material with GEANT4, and evaluating the probability (P_{abs}) of the ${}^3\text{H}$ to be absorbed before decaying. The absorption cross section employed for the simulation has been extracted from Ref. [67], which accounts for the extension of the ${}^3\text{H}$ wave function, and amounts to about 1.5 times that of the ${}^3\text{He}$. The probability of ${}^3\text{H}$ to be absorbed is found to be increasing as a function of p_{T} due to the larger amount of material crossed by the high-momentum particle. The corresponding correction, computed as $C_{\text{abs}} = 1 - P_{\text{abs}}$, ranges from 0.96 to 0.93.

The main systematic uncertainties on the measurement of the ${}^3\text{H}$ p_{T} spectra are due to the ${}^3\text{H}$ decay reconstruction, the BDT selection, and the invariant-mass fit in each p_{T} interval. These systematic uncertainties are estimated as an envelope by employing a multi-trial approach. In this approach, the following elements of the analysis are varied: two different weak-decay vertex-reconstruction methods, two different background datasets for the BDT training, two different fit functions for the ${}^3\text{H}$ signal (a Kernel Density Estimator [68] and the DSCB), three different fit functions for the combinatorial background modelling (polynomial of the first and second order, and an exponential function), and different BDT selection thresholds (giving rise to a $\pm 10\%$ variation of the efficiency around its nominal value). These elements are varied incoherently to populate a distribution of different yields that constitute our trial distribution in each p_{T} and centrality interval. The systematic uncertainty is then estimated as the standard deviation of the obtained distributions and varies from 8% to 34% in different intervals. Since the absorption cross section of ${}^3\text{H}$ is uncertain, an additional uncertainty due to the absorption is evaluated by changing the interaction cross section in the simulation to three times the ${}^3\text{He}$ inelastic cross section with the detector materials. This results in systematic uncertainties of 4%–6%, depending on the p_{T} interval. Another source of the uncertainty originates from the uncertainty on the branching ratio, which amounts to 9% and is common to all the p_{T} and centrality classes.

3. Results and discussions

The ${}^3\text{H}$ p_{T} -differential spectra in different centrality intervals, defined as the average of particles and antiparticles, are shown in Fig. 2 along with the spectra of deuterons, antitritons, and ${}^3\text{He}$ in the corresponding centrality ranges, as measured in Ref. [51]. A simultaneous fit with the Blast-Wave model parameterisation [62] is done with all the shown spectra. The parameters of the combined Blast-Wave fit are listed in Table 1. Notably, the temperature and velocity in the Blast-Wave fit are compatible with those obtained by fitting only light nuclei (d , t , ${}^3\text{He}$, ${}^4\text{He}$) [52], suggesting a similar kinetic freeze-out surface for light-flavoured nuclei.

Individual Blast-Wave fits are employed to extrapolate the ${}^3\text{H}$ spectrum in the unmeasured p_{T} range and obtain the total yield (dN/dy) in the three centrality classes. The variation intervals of the fit parameters are restricted to an interval of $\pm 1\sigma$ around the parameters obtained from the combined fits shown in Fig. 2. The resulting dN/dy values are reported in Table 1. The fraction of extrapolated yield using the Blast-Wave fit is 13%, 39%, and 27% for the 0–10%, 10–30%, and 30–50% centrality classes, respectively. The total uncertainties on the integrated yields $\sigma(\text{BW}_{\text{tot}})$ are computed by fitting the spectra considering both statistical and systematic uncertainties. To separate the statistical and systematic components of the uncertainty which originates from the Blast-Wave extrapolation, a fit considering only statistical uncertainty of the ${}^3\text{H}$ spectra is used to estimate the statistical component ($\sigma(\text{BW}_{\text{stat}})$). The systematic uncertainty due to the fitting procedure is extracted using the relation $\sigma(\text{BW}_{\text{sys}}) = \sqrt{\sigma(\text{BW}_{\text{tot}})^2 - \sigma(\text{BW}_{\text{stat}})^2}$. An additional source of systematic uncertainty to the measured yield arises from the unknown p_{T} distribution of ${}^3\text{H}$. As the fits performed with other functions, namely m_{T} -exponential and Boltzmann, have not passed the Pearson χ^2 test for the goodness of the fit and since the p_{T} distribution of ${}^3\text{H}$ should be very similar to ${}^3\text{He}$ according to the Blast-Wave model [62], the related uncertainty is inherited from the previous ${}^3\text{He}$ production analysis [51] and corresponds to 1.8%, 3.3%, and 0.3% of the measured integrated yield in 0–10%, 10–30%, 30–50%, respectively.

The production yield of ${}^3\text{H}$ provides a powerful tool to investigate the mechanism of nuclear production in relativistic hadronic col-

Table 1

Parameters of the combined Blast-Wave fits and integrated (${}^3\Lambda H + {}^3\bar{\Lambda} H$)/2 yields in different centrality intervals. The fits include deuteron, antitriton, 3He , and ${}^3\Lambda H$ as shown in Fig. 2. The ${}^3\Lambda H$ yields are obtained with an individual Blast-Wave fit whose parameters are restricted in 1σ region of the parameters shown in the table.

Centrality	$\langle \beta_T \rangle$	T (GeV)	n	χ^2 / ndf	$dN/dy \times 10^{-5}$ (B.R. = 0.25)
0–10%	0.694 ± 0.003	0.103 ± 0.005	0.498 ± 0.009	43.4 / 39	$4.83 \pm 0.23(\text{stat}) \pm 0.57(\text{syst})$
10–30%	0.666 ± 0.003	0.132 ± 0.008	0.507 ± 0.012	19.1 / 34	$2.62 \pm 0.25(\text{stat}) \pm 0.40(\text{syst})$
30–50%	0.598 ± 0.005	0.152 ± 0.010	0.660 ± 0.022	21.8 / 33	$1.27 \pm 0.10(\text{stat}) \pm 0.14(\text{syst})$

lisions [18]. The measured ${}^3\Lambda H$ yield in all the centrality intervals is directly compared with the predictions from the grand-canonical SHM [69] with $T = 155$ MeV. The predicted ${}^3\Lambda H dN/dy$ (9.5×10^{-5}) is approximately two times higher than the measured one in central Pb–Pb collisions, suggesting that the SHM, as applied, may lack certain elements necessary for accurately describing the generation of this weakly bound state.

On the other hand, while the SHM is able to calculate directly the absolute yields of hadrons, in the coalescence model only the yield ratios among particles can be computed without any further knowledge of the momentum spectra of the nucleons. To compare with both the models, SHM and coalescence, the ${}^3\Lambda H / {}^3He$ ratio is considered. The 3He production spectra from Ref. [51] are not corrected for the feed-down from ${}^3\Lambda H$. However, this effect is estimated to be at most 1.7%, and a systematic uncertainty of the same magnitude is included in the ratio to account for it. The produced charged-particle multiplicities per unit of pseudorapidity $\langle dN_{\text{ch}}/d\eta \rangle$, which are related to the centrality of the collision and can reflect the size of the fireball, may have effects on the ratios of particle yields and need to be taken into account. In this case, the grand-canonical SHM predicts no multiplicity dependence. A deviation from the grand-canonical ensemble prediction is present in the canonical SHM only for $\langle dN_{\text{ch}}/d\eta \rangle_{|\eta|<0.5} < 100$ [29], which corresponds to peripheral collisions comparatively and is not covered by the presented results. The coalescence model formulation here considered [70] uses the Wigner function formalism and a parametrisation of the wave function of the ${}^3\Lambda H$ that depends on its Λ separation energy, and it was already successfully applied to predict the production of other light nuclei in heavy-ion collisions [71,72]. Three different coalescence predictions are shown by setting B_Λ to the latest ALICE and STAR experimental values and to the world average of the B_Λ measurements [18,20,24]. The uncertainty due to the B_Λ value is asymmetric as the ${}^3\Lambda H$ wave function width is not a linear function of B_Λ . Furthermore, the coalescence model predicts a suppression of the ${}^3\Lambda H / {}^3He$ ratio with decreasing multiplicities due to the interplay between the smaller hadron emission source in peripheral Pb–Pb collisions and the wide wave function of the ${}^3\Lambda H$. In Fig. 3, the model predictions are compared with the measured ${}^3\Lambda H / {}^3He$ yield ratio as a function of the average charged-particle multiplicity of the analysed centrality intervals. The measured ${}^3\Lambda H / {}^3He$ yield ratios are well described by the coalescence prediction using the current world average of B_Λ (solid blue line). In addition, the recent STAR measurements [21] suggest a similar suppression of the ${}^3\Lambda H / {}^3He$ ratio going from large (Au–Au and U–U) to smaller (Zr–Zr and Ru–Ru) collision systems. For larger values of B_Λ , the predictions from the coalescence model approach that of the SHM, but they are not compatible with the measured ratios. The results from a prior ALICE analysis [15] in Pb–Pb collisions at $\sqrt{s_{\text{NN}}} = 2.76$ TeV are included in Fig. 3 for comparison. The results presented in this Letter remain consistent with the previous study within a 2σ confidence interval, but uncertainties are twice as small as those obtained from the smaller data sample at lower collision energy.

In Fig. 4, the ${}^3\Lambda H / {}^3He$ yield ratio as a function of p_T in the three different centrality intervals is shown. While the SHM does not infer the expected p_T shape of the particles, the coalescence mechanism implies a decrease of the ${}^3\Lambda H / {}^3He$ ratio for increasing p_T . Conversely, in a simple hydrodynamic picture like the Blast-Wave model, the radial flow boosts the high p_T production of heavier particles such as the ${}^3\Lambda H$. Consequently, within the Blast-Wave framework, the ${}^3\Lambda H / {}^3He$ ratio is

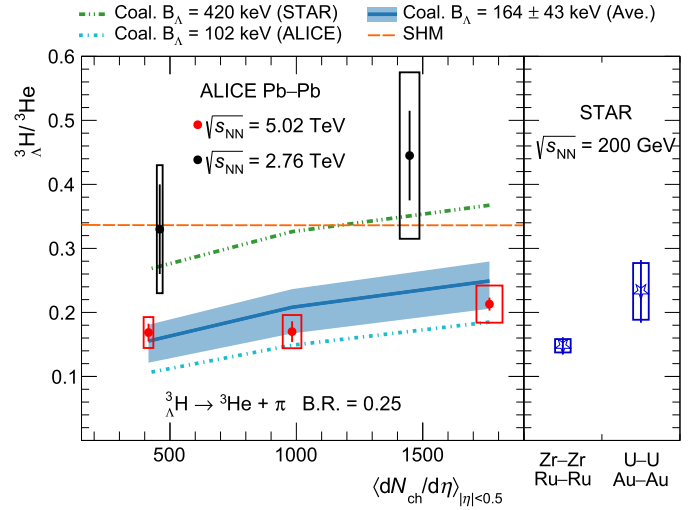


Fig. 3. Yield ratio of ${}^3\Lambda H$ to 3He together with theoretical predictions as a function of multiplicity. In the left panel, the results of this analysis are compared with the ALICE measurement at $\sqrt{s_{\text{NN}}} = 2.76$ TeV [15]. Vertical lines are used for the statistical uncertainties and the height of the boxes for the systematic ones. The width of the boxes refers to the uncertainties of multiplicity. For each centrality interval the $\langle dN_{\text{ch}}/d\eta \rangle$ is taken from Ref. [73] and the 3He yield from Ref. [51]. The dense orange dashed line represents the expectation of SHM, while the other three sets of lines stand for coalescence model with different B_Λ hypotheses. The coalescence prediction with world average B_Λ is displayed with a 1σ uncertainty as the filled area, both lines and shadowed areas are linear interpolations of the available model calculations [70]. In the right panel, the results of recent STAR measurement are shown for comparison [21].

expected to increase as a function of p_T . However, the current experimental uncertainties do not allow for a definitive conclusion on the trend of the ${}^3\Lambda H / {}^3He$ ratio as a function of p_T .

4. Conclusions

This Letter presents the first p_T -differential measurement of the ${}^3\Lambda H$ production in Pb–Pb collisions at $\sqrt{s_{\text{NN}}} = 5.02$ TeV. The p_T distribution of ${}^3\Lambda H$ is well described by a simultaneous Blast-Wave fit with other light nuclei. The fit temperature and velocity profiles are compatible with those found for other light-flavoured nuclei, hinting to a common kinetic freeze-out surface for hypernuclei and ordinary nuclei produced in Pb–Pb collisions. The p_T -integrated yields show a significant discrepancy with respect to the predictions of the SHM tuned to fit the other light-flavoured particles. Furthermore, the yield ratio ${}^3\Lambda H / {}^3He$ was calculated to test the predictions of the coalescence model, that is able to describe the measured ratios when assuming the correct binding energy of the ${}^3\Lambda H$. Finally, both the coalescence and the Blast-Wave models describe the experimental data for the ${}^3\Lambda H / {}^3He$ ratios as a function of p_T . However, their predictions have a different p_T trend. Presently, the large experimental uncertainties preclude a definitive interpretation; however, the forthcoming data from LHC Run 3 will allow the ALICE Collaboration to measure this quantity with unprecedented precision.

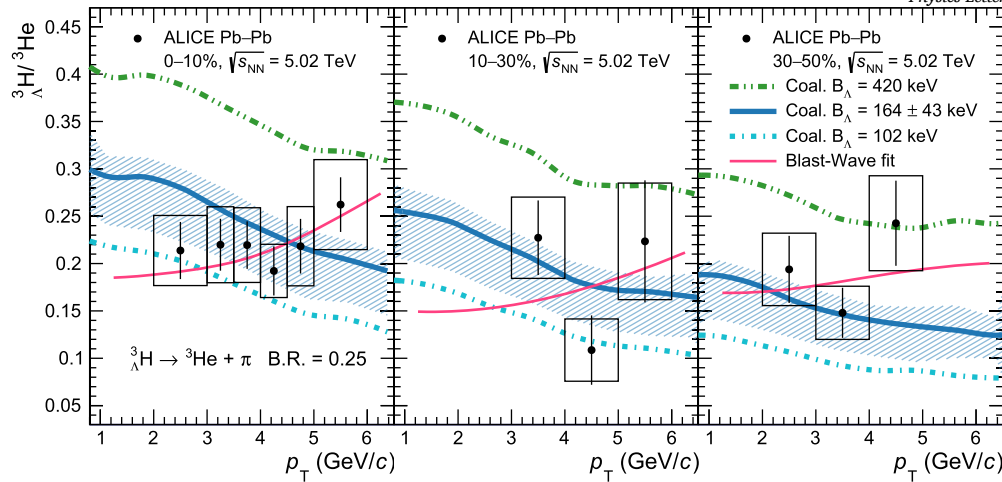


Fig. 4. The ${}^3\text{H}/{}^3\text{He}$ yield ratio together with theoretical predictions in different centrality intervals as a function of p_{T} . The vertical lines and the height of the boxes represent the statistical and systematic uncertainties, respectively. The width of the boxes displays the range of the p_{T} intervals. The pink solid lines are calculated as the ratios of the Blast-Wave fit functions for ${}^3\text{He}$ and ${}^3\text{H}$. The other three curves stand for the predictions of the coalescence model with different B_{Λ} hypotheses. The coalescence prediction with world average B_{Λ} is displayed with a 1σ uncertainty band [70].

Declaration of competing interest

The authors declare that they have no known competing financial interests or personal relationships that could have appeared to influence the work reported in this paper.

Acknowledgements

The ALICE Collaboration would like to thank all its engineers and technicians for their invaluable contributions to the construction of the experiment and the CERN accelerator teams for the outstanding performance of the LHC complex. The ALICE Collaboration gratefully acknowledges the resources and support provided by all Grid centres and the Worldwide LHC Computing Grid (WLCG) collaboration. The ALICE Collaboration acknowledges the following funding agencies for their support in building and running the ALICE detector: A.I. Alikhanyan National Science Laboratory (Yerevan Physics Institute) Foundation (ANSL), State Committee of Science and World Federation of Scientists (WFS), Armenia; Austrian Academy of Sciences, Austrian Science Fund (FWF): [M 2467-N36] and Nationalstiftung für Forschung, Technologie und Entwicklung, Austria; Ministry of Communications and High Technologies, National Nuclear Research Center, Azerbaijan; Conselho Nacional de Desenvolvimento Científico e Tecnológico (CNPq), Financiadora de Estudos e Projetos (Finep), Fundação de Amparo à Pesquisa do Estado de São Paulo (FAPESP) and Universidade Federal do Rio Grande do Sul (UFRGS), Brazil; Bulgarian Ministry of Education and Science, within the National Roadmap for Research Infrastructures 2020–2027 (object CERN), Bulgaria; Ministry of Education of China (MOEC), Ministry of Science & Technology of China (MSTC) and National Natural Science Foundation of China (NSFC), China; Ministry of Science and Education and Croatian Science Foundation, Croatia; Centro de Aplicaciones Tecnológicas y Desarrollo Nuclear (CEADEN), Cubaenergía, Cuba; The Ministry of Education, Youth and Sports of the Czech Republic, Czech Republic; The Danish Council for Independent Research | Natural Sciences, the Villum Fonden and Danish National Research Foundation (DNRF), Denmark; Helsinki Institute of Physics (HIP), Finland; Commissariat à l’Energie Atomique (CEA) and Institut National de Physique Nucléaire et de Physique des Particules (IN2P3) and Centre National de la Recherche Scientifique (CNRS), France; Bundesministerium für Bildung und Forschung (BMBF) and GSI Helmholtzzentrum für Schwerionenforschung GmbH, Germany; General Secretariat for Research and Technology, Ministry of Education, Research and Religions, Greece; National Research, Development and Innovation Office, Hun-

gary; Department of Atomic Energy, Government of India (DAE), Department of Science and Technology, Government of India (DST), University Grants Commission, Government of India (UGC) and Council of Scientific and Industrial Research (CSIR), India; National Research and Innovation Agency - BRIN, Indonesia; Istituto Nazionale di Fisica Nucleare (INFN), Italy; Japanese Ministry of Education, Culture, Sports, Science and Technology (MEXT) and Japan Society for the Promotion of Science (JSPS) KAKENHI, Japan; Consejo Nacional de Ciencia (CONACYT) y Tecnología, through Fondo de Cooperación Internacional en Ciencia y Tecnología (FONCICYT) and Dirección General de Asuntos del Personal Académico (DGAPA), Mexico; Nederlandse Organisatie voor Wetenschappelijk Onderzoek (NWO), Netherlands; The Research Council of Norway, Norway; Pontificia Universidad Católica del Perú, Peru; Ministry of Science and Higher Education, National Science Centre and WUT ID-UB, Poland; Korea Institute of Science and Technology Information and National Research Foundation of Korea (NRF), Republic of Korea; Ministry of Education and Scientific Research, Institute of Atomic Physics, Ministry of Research and Innovation and Institute of Atomic Physics and Universitatea Națională de Știință și Tehnologie Politehnica Bucuresti, Romania; Ministry of Education, Science, Research and Sport of the Slovak Republic, Slovakia; National Research Foundation of South Africa, South Africa; Swedish Research Council (VR) and Knut & Alice Wallenberg Foundation (KAW), Sweden; European Organization for Nuclear Research, Switzerland; Suranaree University of Technology (SUT), National Science and Technology Development Agency (NSTDA) and National Science, Research and Innovation Fund (NSRF via PMU-B B05F650021), Thailand; Turkish Energy, Nuclear and Mineral Research Agency (TENMAK), Turkey; National Academy of Sciences of Ukraine, Ukraine; Science and Technology Facilities Council (STFC), United Kingdom; National Science Foundation of the United States of America (NSF) and United States Department of Energy, Office of Nuclear Physics (DOE NP), United States of America. In addition, individual groups or members have received support from: Czech Science Foundation (grant no. 23-07499S), Czech Republic; European Research Council (grant no. 950692), European Union; ICSC - Centro Nazionale di Ricerca in High Performance Computing, Big Data and Quantum Computing, European Union - NextGenerationEU; Academy of Finland (Center of Excellence in Quark Matter) (grant nos. 346327, 346328), Finland.

Data availability

This manuscript has associated data in a HEPData repository at: <https://www.hepdata.net/record/ins2791616>.

References

- [1] J. Schaffner-Bielich, Hypernuclear physics for neutron stars, Nucl. Phys. A 804 (2008) 309–321, arXiv:0801.3791 [astro-ph].
- [2] L. Tolos, L. Fabbietti, Strangeness in nuclei and neutron stars, Prog. Part. Nucl. Phys. 112 (2020) 103770, arXiv:2002.09223 [nucl-ex].
- [3] D. Lonardoni, A. Lovato, S. Gandolfi, F. Pederiva, Hyperon puzzle: hints from quantum Monte Carlo calculations, Phys. Rev. Lett. 114 (2015) 092301, arXiv:1407.4448 [nucl-th].
- [4] D. Logoteta, I. Vidana, I. Bombaci, Impact of chiral hyperonic three-body forces on neutron stars, Eur. Phys. J. A 55 (2019) 207, arXiv:1906.11722 [nucl-th].
- [5] L. Fabbietti, V. Mantovani Sarti, O. Vazquez Doce, Study of the strong interaction among hadrons with correlations at the LHC, Annu. Rev. Nucl. Part. Sci. 71 (2021) 377–402, arXiv:2012.09806 [nucl-ex].
- [6] ALICE Collaboration, S. Acharya, et al., Unveiling the strong interaction among hadrons at the LHC, Nature 588 (2020) 232–238, arXiv:2005.11495 [nucl-ex], Erratum: Nature 590 (2021) E13.
- [7] H. Kamada, J. Golak, K. Miyagawa, H. Witala, W. Gloeckle, π -mesonic decay of the hypertriton, Phys. Rev. C 57 (1998) 1595–1603, arXiv:nucl-th/9709035.
- [8] J. Haidenbauer, U.G. Meißner, A. Nogga, Hyperon–nucleon interaction within chiral effective field theory revisited, Eur. Phys. J. A 56 (2020) 91, arXiv:1906.11681 [nucl-th].
- [9] D. Lonardoni, F. Pederiva, Medium-mass hypernuclei and the nucleon-isospin dependence of the three-body hyperon-nucleon-nucleon force, arXiv:1711.07521 [nucl-th].
- [10] R.J. Prem, P.H. Steinberg, Lifetimes of hypernuclei, ${}^3_{\Lambda}\text{H}$, ${}^4_{\Lambda}\text{H}$, ${}^5_{\Lambda}\text{H}$, Phys. Rev. 136 (1964) B1803–B1806, Publisher: American Physical Society.
- [11] G. Keyes, et al., New measurement of the ${}^3_{\Lambda}\text{H}$ lifetime, Phys. Rev. Lett. 20 (1968) 819–821.
- [12] R.E. Phillips, J. Schneps, Lifetimes of light hyperfragments. II, Phys. Rev. 180 (1969) 1307–1318.
- [13] G. Bohm, et al., On the lifetime of the ${}^3_{\Lambda}\text{H}$ hypernucleus, Nucl. Phys. B 16 (1970) 46–52, Erratum: Nucl. Phys. B 16 (1970) 523.
- [14] G. Keyes, J. Sacton, J.H. Wickens, M.M. Block, A measurement of the lifetime of the ${}^3_{\Lambda}\text{H}$ hypernucleus, Nucl. Phys. B 67 (1973) 269–283.
- [15] ALICE Collaboration, J. Adam, et al., ${}^3_{\Lambda}\text{H}$ and ${}^3_{\Lambda}\overline{\text{H}}$ production in Pb–Pb collisions at $\sqrt{s_{\text{NN}}} = 2.76$ TeV, Phys. Lett. B 754 (2016) 360–372, arXiv:1506.08453 [nucl-ex].
- [16] ALICE Collaboration, S. Acharya, et al., ${}^3_{\Lambda}\text{H}$ and ${}^3_{\Lambda}\overline{\text{H}}$ lifetime measurement in Pb–Pb collisions at $\sqrt{s_{\text{NN}}} = 5.02$ TeV via two-body decay, Phys. Lett. B 797 (2019) 134905, arXiv:1907.06906 [nucl-ex].
- [17] ALICE Collaboration, S. Acharya, et al., Hypertriton production in p–Pb collisions at $\sqrt{s_{\text{NN}}} = 5.02$ TeV, Phys. Rev. Lett. 128 (2022) 252003, arXiv:2107.10627 [nucl-ex].
- [18] ALICE Collaboration, S. Acharya, et al., Measurement of the lifetime and Λ separation energy of ${}^3_{\Lambda}\text{H}$, Phys. Rev. Lett. 131 (2023) 102302, arXiv:2209.07360 [nucl-ex].
- [19] STAR Collaboration, L. Adamczyk, et al., Measurement of the ${}^3_{\Lambda}\text{H}$ lifetime in Au+Au collisions at the BNL relativistic heavy ion collider, Phys. Rev. C 97 (2018) 054909, arXiv:1710.00436 [nucl-ex].
- [20] STAR Collaboration, M. Abdallah, et al., Measurements of ${}^3_{\Lambda}\text{H}$ and ${}^4_{\Lambda}\text{H}$ lifetimes and yields in Au+Au collisions in the high baryon density region, Phys. Rev. Lett. 128 (2022) 202301, arXiv:2110.09513 [nucl-ex].
- [21] STAR Collaboration, Observation of the antimatter hypernucleus ${}^4_{\Lambda}\overline{\text{H}}$, arXiv:2310.12674 [nucl-ex].
- [22] J. Chen, X. Dong, Y.-G. Ma, Z. Xu, Measurements of the lightest hypernucleus (${}^3_{\Lambda}\text{H}$): progress and perspective, Sci. Bull. 68 (2023) 3252–3260, arXiv:2311.09877 [nucl-ex].
- [23] Y.-G. Ma, Hypernuclei as a laboratory to test hyperon–nucleon interactions, Nucl. Sci. Tech. 34 (2023) 97.
- [24] P. Eckert, et al., Chart of hypernuclides — hypernuclear structure and decay data, <https://hypernuclei.kph.uni-mainz.de>, 2023.
- [25] A. Cobis, A.S. Jensen, D.V. Fedorov, The simplest strange three-body halo, J. Phys. G, Nucl. Part. Phys. 23 (1997) 401.
- [26] H. Nemura, Y. Suzuki, Y. Fujiwara, C. Nakamoto, Study of light Λ - and $\Lambda\Lambda$ -hypernuclei with the stochastic variational method and effective AN potentials, Prog. Theor. Phys. 103 (2000) 929–958, arXiv:nucl-th/9912065 [nucl-th].
- [27] F. Hildenbrand, H.W. Hammer, Three-body hypernuclei in pionless effective field theory, Phys. Rev. C 100 (2019) 034002, arXiv:1904.05818 [nucl-th], Erratum: Phys. Rev. C 102 (2020) 039901.
- [28] A. Andronic, P. Braun-Munzinger, K. Redlich, J. Stachel, Decoding the phase structure of QCD via particle production at high energy, Nature 561 (2018) 321–330, arXiv:1710.09425 [nucl-th].
- [29] V. Vovchenko, B. Dönigus, H. Stoecker, Multiplicity dependence of light nuclei production at LHC energies in the canonical statistical model, Phys. Lett. B 785 (2018) 171–174, arXiv:1808.05245 [hep-ph].
- [30] V. Vovchenko, B. Dönigus, H. Stoecker, Canonical statistical model analysis of p–p, p–Pb, and Pb–Pb collisions at energies available at the CERN large hadron collider, Phys. Rev. C 100 (2019) 054906, arXiv:1906.03145 [hep-ph].
- [31] V. Vovchenko, V. Koch, Centrality dependence of proton and light nuclei yields as a consequence of baryon annihilation in the hadronic phase, Phys. Lett. B 835 (2022) 137577, arXiv:2210.15641 [nucl-th].
- [32] N. Sharma, L. Kumar, P.M. Lo, K. Redlich, Light-nuclei production in pp and pA collisions in the baryon canonical ensemble approach, Phys. Rev. C 107 (2023) 054903, arXiv:2210.15617 [nucl-th].
- [33] L.-W. Chen, C.M. Ko, B.-A. Li, Light cluster production in intermediate-energy heavy ion collisions induced by neutron rich nuclei, Nucl. Phys. A 729 (2003) 809–834, arXiv:nucl-th/0306032.
- [34] K. Blum, K.C.Y. Ng, R. Sato, M. Takimoto, Cosmic rays, antihelium, and an old navy spotlight, Phys. Rev. D 96 (2017) 103021, arXiv:1704.05431 [astro-ph.HE].
- [35] F. Bellini, A.P. Kalweit, Testing coalescence and statistical-thermal production scenarios for (anti-) hyper-nuclei and exotic QCD objects at LHC energies, Phys. Rev. C 99 (2019) 054905, arXiv:1807.05894 [hep-ph].
- [36] K.-J. Sun, C.M. Ko, B. Dönigus, Suppression of light nuclei production in collisions of small systems at the large hadron collider, Phys. Lett. B 792 (2019) 132–137, arXiv:1812.05175 [nucl-th].
- [37] F. Bellini, K. Blum, A.P. Kalweit, M. Puccio, Examination of coalescence as the origin of nuclei in hadronic collisions, Phys. Rev. C 103 (2021) 014907, arXiv:2007.01750 [nucl-th].
- [38] M. Kachelriess, S. Ostapchenko, J. Tjemsland, On nuclear coalescence in small interacting systems, Eur. Phys. J. A 57 (2021) 167, arXiv:2012.04352 [hep-ph].
- [39] M. Mahlein, et al., A realistic coalescence model for deuteron production, Eur. Phys. J. C 83 (2023) 804, arXiv:2302.12696 [hep-ex].
- [40] R. Scheibl, U.W. Heinz, Coalescence and flow in ultrarelativistic heavy ion collisions, Phys. Rev. C 59 (1999) 1585–1602, arXiv:nucl-th/9809092.
- [41] ALICE Collaboration, J. Adam, et al., Production of light nuclei and anti-nuclei in pp and Pb–Pb collisions at energies available at the CERN large hadron collider, Phys. Rev. C 93 (2016) 024917, arXiv:1506.08951 [nucl-ex].
- [42] ALICE Collaboration, S. Acharya, et al., Production of deuterons, tritons, ${}^3_{\Lambda}\text{He}$ nuclei and their antinuclei in pp collisions at $\sqrt{s} = 0.9$, 2.76 and 7 TeV, Phys. Rev. C 97 (2018) 024615, arXiv:1709.08522 [nucl-ex].
- [43] ALICE Collaboration, S. Acharya, et al., Production of ${}^4_{\Lambda}\text{He}$ and ${}^4_{\Lambda}\overline{\text{He}}$ in Pb–Pb collisions at $\sqrt{s_{\text{NN}}} = 2.76$ TeV at the LHC, Nucl. Phys. A 971 (2018) 1–20, arXiv:1710.07531 [nucl-ex].
- [44] ALICE Collaboration, S. Acharya, et al., Measurement of deuteron spectra and elliptic flow in Pb–Pb collisions at $\sqrt{s_{\text{NN}}} = 2.76$ TeV at the LHC, Eur. Phys. J. C 77 (2017) 658, arXiv:1707.07304 [nucl-ex].
- [45] ALICE Collaboration, S. Acharya, et al., Multiplicity dependence of (anti-)deuteron production in pp collisions at $\sqrt{s} = 7$ TeV, Phys. Lett. B 794 (2019) 50–63, arXiv:1902.09290 [nucl-ex].
- [46] ALICE Collaboration, S. Acharya, et al., Production of (anti-) ${}^3_{\Lambda}\text{He}$ and (anti-) ${}^3_{\Lambda}\overline{\text{H}}$ in p–Pb collisions at $\sqrt{s_{\text{NN}}} = 5.02$ TeV, Phys. Rev. C 101 (2020) 044906, arXiv:1910.14401 [nucl-ex].
- [47] ALICE Collaboration, S. Acharya, et al., (Anti-)deuteron production in pp collisions at $\sqrt{s} = 13$ TeV, Eur. Phys. J. C 80 (2020) 889, arXiv:2003.03184 [nucl-ex].
- [48] ALICE Collaboration, S. Acharya, et al., Measurement of the production of (anti)nuclei in p–Pb collisions at $\sqrt{s_{\text{NN}}} = 8.16$ TeV, Phys. Lett. B 846 (2023) 137795, arXiv:2212.04777 [nucl-ex].
- [49] ALICE Collaboration, S. Acharya, et al., Production of light (anti)nuclei in pp collisions at $\sqrt{s} = 13$ TeV, J. High Energy Phys. 01 (2022) 106, arXiv:2109.13026 [nucl-ex].
- [50] ALICE Collaboration, S. Acharya, et al., Production of light (anti)nuclei in pp collisions at $\sqrt{s} = 5.02$ TeV, Eur. Phys. J. C 82 (2022) 289, arXiv:2112.00610 [nucl-ex].
- [51] ALICE Collaboration, S. Acharya, et al., Light (anti)nuclei production in Pb–Pb collisions at $\sqrt{s_{\text{NN}}} = 5.02$ TeV, Phys. Rev. C 107 (2023) 064904, arXiv:2211.14015 [nucl-ex].
- [52] ALICE Collaboration, S. Acharya, et al., Measurement of (anti)alpha production in central Pb–Pb collisions at $\sqrt{s_{\text{NN}}} = 5.02$ TeV, arXiv:2311.11758 [nucl-ex].
- [53] S. Mrowczynski, Production of light nuclei at colliders – coalescence vs. thermal model, Eur. Phys. J. Spec. Top. 229 (2020) 3559–3583, arXiv:2004.07029 [nucl-th].
- [54] J. Rais, H. van Hees, C. Greiner, Bound-state formation in time-dependent potentials, Phys. Rev. C 106 (2022) 064004, arXiv:2207.04898 [quant-ph].
- [55] ALICE Collaboration, B.B. Abelev, et al., Performance of the ALICE experiment at the CERN LHC, Int. J. Mod. Phys. A 29 (2014) 1430044, arXiv:1402.4476 [nucl-ex].
- [56] ALICE Collaboration, K. Aamodt, et al., Alignment of the ALICE inner tracking system with cosmic-ray tracks, J. Instrum. 5 (2010) P03003, arXiv:1001.0502 [physics.ins-det].
- [57] J. Alme, et al., The ALICE TPC, a large 3-dimensional tracking device with fast read-out for ultra-high multiplicity events, Nucl. Instrum. Methods A 622 (2010) 316–367.
- [58] ALICE Collaboration, E. Abbas, et al., Performance of the ALICE VZERO system, J. Instrum. 8 (2013) P10016, arXiv:1306.3130 [nucl-ex].
- [59] ALICE Collaboration, Centrality determination in heavy ion collisions, ALICE-PUBLIC-2018-011, <https://cds.cern.ch/record/2636623>, 2018.
- [60] ALICE Collaboration, S. Acharya, et al., Measurements of chemical potentials in Pb–Pb collisions at $\sqrt{s_{\text{NN}}} = 5.02$ TeV, arXiv:2311.13332 [nucl-ex].
- [61] X.-N. Wang, M. Gyulassy, HIJING: a Monte Carlo model for multiple jet production in pp, pA and AA collisions, Phys. Rev. D 44 (1991) 3501–3516.
- [62] E. Schnedermann, J. Sollfrank, U.W. Heinz, Thermal phenomenology of hadrons from 200 AGeV S+S collisions, Phys. Rev. C 48 (1993) 2462–2475, arXiv:nucl-th/9307020.
- [63] GEANT4 Collaboration, S. Agostinelli, et al., GEANT4—a simulation toolkit, Nucl. Instrum. Methods A 506 (2003) 250–303.

- [64] T. Chen, C. Guestrin, Xgboost: a scalable tree boosting system, in: Proceedings of the 22nd ACM SIGKDD International Conference on Knowledge Discovery and Data Mining, KDD '16, Association for Computing Machinery, New York, NY, USA, 2016, pp. 785–794.
- [65] L. Barioglio, F. Catalano, M. Concas, P. Fecchio, F. Grossa, F. Mazzaschi, M. Puccio, hipe4ml/hipe4ml, <https://doi.org/10.5281/zenodo.5734093>, Nov., 2021.
- [66] W. Verkerke, D.P. Kirkby, The RooFit toolkit for data modeling, eConf C0303241 (2003) MOLT007, arXiv:physics/0306116, <https://root.cern.ch/doc/master/classRooCrystalBall.html>.
- [67] M.V. Evlanov, A.M. Sokolov, V.K. Tartakovskiy, S.A. Khorozov, Y. Lukstishin, Interaction of hypertritons with nuclei at high-energies, Nucl. Phys. A 632 (1998) 624–632.
- [68] K. Cranmer, Kernel estimation in high-energy physics, Comput. Phys. Commun. 136 (2001) 198–207.
- [69] V. Vovchenko, H. Stoecker, Thermal-FIST: a package for heavy-ion collisions and hadronic equation of state, Comput. Phys. Commun. 244 (2019) 295–310, arXiv: 1901.05249 [nucl-th].
- [70] D.-N. Liu, et al., Softening of the hypertriton transverse momentum spectrum in heavy-ion collisions, Phys. Lett. B 855 (2024) 138855, arXiv:2404.02701 [nucl-th].
- [71] W. Zhao, K.-j. Sun, C.M. Ko, X. Luo, Multiplicity scaling of light nuclei production in relativistic heavy-ion collisions, Phys. Lett. B 820 (2021) 136571, arXiv:2105.14204 [nucl-th].
- [72] K.-J. Sun, C.M. Ko, Event-by-event antideuteron multiplicity fluctuation in Pb+Pb collisions at $\sqrt{s_{NN}} = 5.02$ TeV, Phys. Lett. B 840 (2023) 137864, arXiv:2204.10879 [nucl-th].
- [73] ALICE Collaboration, J. Adam, et al., Centrality dependence of the charged-particle multiplicity density at midrapidity in Pb–Pb collisions at $\sqrt{s_{NN}} = 5.02$ TeV, Phys. Rev. Lett. 116 (2016) 222302, arXiv:1512.06104 [nucl-ex].

ALICE Collaboration

- S. Acharya ^{127, ID}, D. Adamová ^{86, ID}, A. Agarwal ¹³⁵, G. Aglieri Rinella ^{32, ID}, L. Aglietta ^{24, ID}, M. Agnello ^{29, ID}, N. Agrawal ^{25, ID}, Z. Ahammed ^{135, ID}, S. Ahmad ^{15, ID}, S.U. Ahn ^{71, ID}, I. Ahuja ^{37, ID}, A. Akindinov ^{141, ID}, V. Akishina ³⁸, M. Al-Turany ^{97, ID}, D. Aleksandrov ^{141, ID}, B. Alessandro ^{56, ID}, H.M. Alfanda ^{6, ID}, R. Alfaro Molina ^{67, ID}, B. Ali ^{15, ID}, A. Alici ^{25, ID}, N. Alizadehvandchali ^{116, ID}, A. Alkin ^{104, ID}, J. Alme ^{20, ID}, G. Alocco ^{52, ID}, T. Alt ^{64, ID}, A.R. Altamura ^{50, ID}, I. Altsybeev ^{95, ID}, J.R. Alvarado ^{44, ID}, C.O.R. Alvarez ⁴⁴, M.N. Anaam ^{6, ID}, C. Andrei ^{45, ID}, N. Andreou ^{115, ID}, A. Andronic ^{126, ID}, E. Andronov ^{141, ID}, V. Anguelov ^{94, ID}, F. Antinori ^{54, ID}, P. Antonioli ^{51, ID}, N. Apadula ^{74, ID}, L. Aphecetche ^{103, ID}, H. Appelshäuser ^{64, ID}, C. Arata ^{73, ID}, S. Arcelli ^{25, ID}, M. Aresti ^{22, ID}, R. Arnaldi ^{56, ID}, J.G.M.C.A. Arneiro ^{110, ID}, I.C. Arsene ^{19, ID}, M. Arslanbekci ^{138, ID}, A. Augustinus ^{32, ID}, R. Averbeck ^{97, ID}, D. Averyanov ^{141, ID}, M.D. Azmi ^{15, ID}, H. Baba ¹²⁴, A. Badalà ^{53, ID}, J. Bae ^{104, ID}, Y.W. Baek ^{40, ID}, X. Bai ^{120, ID}, R. Bailhache ^{64, ID}, Y. Bailung ^{48, ID}, R. Bala ^{91, ID}, A. Balbino ^{29, ID}, A. Baldissari ^{130, ID}, B. Balis ^{2, ID}, D. Banerjee ^{4, ID}, Z. Banoo ^{91, ID}, V. Barbasova ³⁷, F. Barile ^{31, ID}, L. Barioglio ^{56, ID}, M. Barlou ⁷⁸, B. Barman ⁴¹, G.G. Barnaföldi ^{46, ID}, L.S. Barnby ^{115, ID}, E. Barreau ^{103, ID}, V. Barret ^{127, ID}, L. Barreto ^{110, ID}, C. Bartels ^{119, ID}, K. Barth ^{32, ID}, E. Bartsch ^{64, ID}, N. Bastid ^{127, ID}, S. Basu ^{75, ID}, G. Batigne ^{103, ID}, D. Battistini ^{95, ID}, B. Batyunya ^{142, ID}, D. Bauri ⁴⁷, J.L. Bazo Alba ^{101, ID}, I.G. Bearden ^{83, ID}, C. Beattie ^{138, ID}, P. Becht ^{97, ID}, D. Behera ^{48, ID}, I. Belikov ^{129, ID}, A.D.C. Bell Hechavarria ^{126, ID}, F. Bellini ^{25, ID}, R. Bellwied ^{116, ID}, S. Belokurova ^{141, ID}, L.G.E. Beltran ^{109, ID}, Y.A.V. Beltran ^{44, ID}, G. Bencedi ^{46, ID}, A. Bensaoula ¹¹⁶, S. Beole ^{24, ID}, Y. Berdnikov ^{141, ID}, A. Berdnikova ^{94, ID}, L. Bergmann ^{94, ID}, M.G. Besoiu ^{63, ID}, L. Betev ^{32, ID}, P.P. Bhaduri ^{135, ID}, A. Bhasin ^{91, ID}, B. Bhattacharjee ^{41, ID}, L. Bianchi ^{24, ID}, N. Bianchi ^{49, ID}, J. Bielčík ^{35, ID}, J. Bielčíková ^{86, ID}, A.P. Bigot ^{129, ID}, A. Bilandzic ^{95, ID}, G. Biro ^{46, ID}, S. Biswas ^{4, ID}, N. Bize ^{103, ID}, J.T. Blair ^{108, ID}, D. Blau ^{141, ID}, M.B. Blidaru ^{97, ID}, N. Bluhme ³⁸, C. Blume ^{64, ID}, G. Boca ^{21, 55, ID}, F. Bock ^{87, ID}, T. Bodova ^{20, ID}, J. Bok ^{16, ID}, L. Boldizsár ^{46, ID}, M. Bombara ^{37, ID}, P.M. Bond ^{32, ID}, G. Bonomi ^{134, 55, ID}, H. Borel ^{130, ID}, A. Borissov ^{141, ID}, A.G. Borquez Carcamo ^{94, ID}, H. Bossi ^{138, ID}, E. Botta ^{24, ID}, Y.E.M. Bouziani ^{64, ID}, L. Bratrud ^{64, ID}, P. Braun-Munzinger ^{97, ID}, M. Bregant ^{110, ID}, M. Broz ^{35, ID}, G.E. Bruno ^{96, 31, ID}, V.D. Buchakchiev ^{36, ID}, M.D. Buckland ^{23, ID}, D. Budnikov ^{141, ID}, H. Buesching ^{64, ID}, S. Bufalino ^{29, ID}, P. Buhler ^{102, ID}, N. Burmasov ^{141, ID}, Z. Buthelezi ^{68, 123, ID}, A. Bylinkin ^{20, ID}, S.A. Bysiak ¹⁰⁷, J.C. Cabanillas Noris ^{109, ID}, M.F.T. Cabrera ¹¹⁶, M. Cai ^{6, ID}, H. Caines ^{138, ID}, A. Caliva ^{28, ID}, E. Calvo Villar ^{101, ID}, J.M.M. Camacho ^{109, ID}, P. Camerini ^{23, ID}, F.D.M. Canedo ^{110, ID}, S.L. Cantway ^{138, ID}, M. Carabas ^{113, ID}, A.A. Carballo ^{32, ID}, F. Carnesecchi ^{32, ID}, R. Caron ^{128, ID}, L.A.D. Carvalho ^{110, ID}, J. Castillo Castellanos ^{130, ID}, M. Castoldi ^{32, ID}, F. Catalano ^{32, ID}, S. Cattaruzzi ^{23, ID}, C. Ceballos Sanchez ^{142, ID}, R. Cerri ^{24, ID}, I. Chakaberia ^{74, ID}, P. Chakraborty ^{136, 47, ID}, S. Chandra ^{135, ID}, S. Chapelard ^{32, ID}, M. Chartier ^{119, ID}, S. Chattopadhyay ¹³⁵, S. Chattopadhyay ^{135, ID}, S. Chattpadhyay ^{99, ID}, M. Chen ³⁹, T. Cheng ^{97, 6, ID}, C. Cheshkov ^{128, ID}, V. Chibante Barroso ^{32, ID}, D.D. Chinellato ^{111, ID}, E.S. Chizzali ^{95, ID, II}, J. Cho ^{58, ID}, S. Cho ^{58, ID}, P. Chochula ^{32, ID}, Z.A. Chochulska ¹³⁶,

- D. Choudhury ⁴¹, P. Christakoglou ^{84, ID}, C.H. Christensen ^{83, ID}, P. Christiansen ^{75, ID}, T. Chujo ^{125, ID},
 M. Ciacco ^{29, ID}, C. Cicalo ^{52, ID}, M.R. Ciupek ⁹⁷, G. Clai ^{51, III}, F. Colamaria ^{50, ID}, J.S. Colburn ¹⁰⁰, D. Colella ^{31, ID},
 M. Colocci ^{25, ID}, M. Concas ^{32, ID}, G. Conesa Balbastre ^{73, ID}, Z. Conesa del Valle ^{131, ID}, G. Contin ^{23, ID},
 J.G. Contreras ^{35, ID}, M.L. Coquet ^{103, 130, ID}, P. Cortese ^{133, 56, ID}, M.R. Cosentino ^{112, ID}, F. Costa ^{32, ID},
 S. Costanza ^{21, 55, ID}, C. Cot ^{131, ID}, J. Crkovská ^{94, ID}, P. Crochet ^{127, ID}, R. Cruz-Torres ^{74, ID}, P. Cui ^{6, ID},
 M.M. Czarnynoga ¹³⁶, A. Dainese ^{54, ID}, G. Dange ³⁸, M.C. Danisch ^{94, ID}, A. Danu ^{63, ID}, P. Das ^{80, ID}, P. Das ^{4, ID},
 S. Das ^{4, ID}, A.R. Dash ^{126, ID}, S. Dash ^{47, ID}, A. De Caro ^{28, ID}, G. de Cataldo ^{50, ID}, J. de Cuveland ³⁸, A. De Falco ^{22, ID},
 D. De Gruttola ^{28, ID}, N. De Marco ^{56, ID}, C. De Martin ^{23, ID}, S. De Pasquale ^{28, ID}, R. Deb ^{134, ID}, R. Del Grande ^{95, ID},
 L. Dello Stritto ^{32, ID}, W. Deng ^{6, ID}, K.C. Devereaux ¹⁸, P. Dhankher ^{18, ID}, D. Di Bari ^{31, ID}, A. Di Mauro ^{32, ID},
 B. Diab ^{130, ID}, R.A. Diaz ^{142, 7, ID}, T. Dietel ^{114, ID}, Y. Ding ^{6, ID}, J. Ditzel ^{64, ID}, R. Divià ^{32, ID}, Ø. Djupsland ²⁰,
 U. Dmitrieva ^{141, ID}, A. Dobrin ^{63, ID}, B. Dönigus ^{64, ID}, J.M. Dubinski ^{136, ID}, A. Dubla ^{97, ID}, P. Dupieux ^{127, ID},
 N. Dzalaiova ¹³, T.M. Eder ^{126, ID}, R.J. Ehlers ^{74, ID}, F. Eisenhut ^{64, ID}, R. Ejima ^{92, ID}, D. Elia ^{50, ID}, B. Erazmus ^{103, ID},
 F. Ercolelli ^{25, ID}, B. Espagnon ^{131, ID}, G. Eulisse ^{32, ID}, D. Evans ^{100, ID}, S. Evdokimov ^{141, ID}, L. Fabbietti ^{95, ID},
 M. Faggin ^{23, ID}, J. Faivre ^{73, ID}, F. Fan ^{6, ID}, W. Fan ^{74, ID}, A. Fantoni ^{49, ID}, M. Fasel ^{87, ID}, A. Feliciello ^{56, ID},
 G. Feofilov ^{141, ID}, A. Fernández Téllez ^{44, ID}, L. Ferrandi ^{110, ID}, M.B. Ferrer ^{32, ID}, A. Ferrero ^{130, ID},
 C. Ferrero ^{56, ID, IV}, A. Ferretti ^{24, ID}, V.J.G. Feuillard ^{94, ID}, V. Filova ^{35, ID}, D. Finogeev ^{141, ID}, F.M. Fionda ^{52, ID},
 E. Flatland ³², F. Flor ^{138, 116, ID}, A.N. Flores ^{108, ID}, S. Foertsch ^{68, ID}, I. Fokin ^{94, ID}, S. Fokin ^{141, ID}, U. Follo ^{56, ID, IV},
 E. Fragiocomo ^{57, ID}, E. Frajna ^{46, ID}, U. Fuchs ^{32, ID}, N. Funicello ^{28, ID}, C. Furget ^{73, ID}, A. Furs ^{141, ID},
 T. Fusayasu ^{98, ID}, J.J. Gaardhøje ^{83, ID}, M. Gagliardi ^{24, ID}, A.M. Gago ^{101, ID}, T. Gahlaud ⁴⁷, C.D. Galvan ^{109, ID},
 D.R. Gangadharan ^{116, ID}, P. Ganoti ^{78, ID}, C. Garabatos ^{97, ID}, J.M. Garcia ⁴⁴, T. García Chávez ^{44, ID},
 E. Garcia-Solis ^{9, ID}, C. Gargiulo ^{32, ID}, P. Gasik ^{97, ID}, H.M. Gaur ³⁸, A. Gautam ^{118, ID}, M.B. Gay Ducati ^{66, ID},
 M. Germain ^{103, ID}, R.A. Gernhaeuser ⁹⁵, C. Ghosh ¹³⁵, M. Giacalone ^{51, ID}, G. Gioachin ^{29, ID}, S.K. Giri ¹³⁵,
 P. Giubellino ^{97, 56, ID}, P. Giubilato ^{27, ID}, A.M.C. Glaenzer ^{130, ID}, P. Glässel ^{94, ID}, E. Glimos ^{122, ID}, D.J.Q. Goh ⁷⁶,
 V. Gonzalez ^{137, ID}, P. Gordeev ^{141, ID}, M. Gorgon ^{2, ID}, K. Goswami ^{48, ID}, S. Gotovac ³³, V. Grabski ^{67, ID},
 L.K. Graczykowski ^{136, ID}, E. Grecka ^{86, ID}, A. Grelli ^{59, ID}, C. Grigoras ^{32, ID}, V. Grigoriev ^{141, ID}, S. Grigoryan ^{142, 1, ID},
 F. Grossa ^{32, ID}, J.F. Grosse-Oetringhaus ^{32, ID}, R. Grossos ^{97, ID}, D. Grund ^{35, ID}, N.A. Grunwald ⁹⁴,
 G.G. Guardiano ^{111, ID}, R. Guernane ^{73, ID}, M. Guilbaud ^{103, ID}, K. Gulbrandsen ^{83, ID}, J.J.W.K. Gumprecht ¹⁰²,
 T. Gündem ^{64, ID}, T. Gunji ^{124, ID}, W. Guo ^{6, ID}, A. Gupta ^{91, ID}, R. Gupta ^{91, ID}, R. Gupta ^{48, ID}, K. Gwizdziel ^{136, ID},
 L. Gyulai ^{46, ID}, C. Hadjidakis ^{131, ID}, F.U. Haider ^{91, ID}, S. Haidlova ^{35, ID}, M. Haldar ⁴, H. Hamagaki ^{76, ID},
 A. Hamdi ^{74, ID}, Y. Han ^{139, ID}, B.G. Hanley ^{137, ID}, R. Hannigan ^{108, ID}, J. Hansen ^{75, ID}, M.R. Haque ^{97, ID},
 J.W. Harris ^{138, ID}, A. Harton ^{9, ID}, M.V. Hartung ^{64, ID}, H. Hassan ^{117, ID}, D. Hatzifotiadou ^{51, ID}, P. Hauer ^{42, ID},
 L.B. Havener ^{138, ID}, E. Hellbär ^{97, ID}, H. Helstrup ^{34, ID}, M. Hemmer ^{64, ID}, T. Herman ^{35, ID}, S.G. Hernandez ¹¹⁶,
 G. Herrera Corral ^{8, ID}, S. Herrmann ^{128, ID}, K.F. Hetland ^{34, ID}, B. Heybeck ^{64, ID}, H. Hillemanns ^{32, ID},
 B. Hippolyte ^{129, ID}, F.W. Hoffmann ^{70, ID}, B. Hofman ^{59, ID}, G.H. Hong ^{139, ID}, M. Horst ^{95, ID}, A. Horzyk ^{2, ID},
 Y. Hou ^{6, ID}, P. Hristov ^{32, ID}, P. Huhn ⁶⁴, L.M. Huhta ^{117, ID}, T.J. Humanic ^{88, ID}, A. Hutson ^{116, ID}, D. Hutter ^{38, ID},
 M.C. Hwang ^{18, ID}, R. Ilkaev ¹⁴¹, M. Inaba ^{125, ID}, G.M. Innocenti ^{32, ID}, M. Ippolitov ^{141, ID}, A. Isakov ^{84, ID},
 T. Isidori ^{118, ID}, M.S. Islam ^{99, ID}, S. Iurchenko ¹⁴¹, M. Ivanov ¹³, M. Ivanov ^{97, ID}, V. Ivanov ^{141, ID},
 K.E. Iversen ^{75, ID}, M. Jablonski ^{2, ID}, B. Jacak ^{18, 74, ID}, N. Jacazio ^{25, ID}, P.M. Jacobs ^{74, ID}, S. Jadlovska ¹⁰⁶,
 J. Jadlovsky ¹⁰⁶, S. Jaelani ^{82, ID}, C. Jahnke ^{110, ID}, M.J. Jakubowska ^{136, ID}, M.A. Janik ^{136, ID}, T. Janson ⁷⁰,
 S. Ji ^{16, ID}, S. Jia ^{10, ID}, A.A.P. Jimenez ^{65, ID}, F. Jonas ^{74, ID}, D.M. Jones ^{119, ID}, J.M. Jowett ^{32, 97, ID}, J. Jung ^{64, ID},
 M. Jung ^{64, ID}, A. Junique ^{32, ID}, A. Jusko ^{100, ID}, J. Kaewjai ¹⁰⁵, P. Kalinak ^{60, ID}, A. Kalweit ^{32, ID}, A. Karasu
 Uysal ^{72, ID, V}, D. Karatovic ^{89, ID}, N. Karatzenis ¹⁰⁰, O. Karavichev ^{141, ID}, T. Karavicheva ^{141, ID}, E. Karpechev ^{141, ID},

- M.J. Karwowska ^{32,136, ID}, U. Kebschull ^{70, ID}, R. Keidel ^{140, ID}, M. Keil ^{32, ID}, B. Ketzer ^{42, ID}, S.S. Khade ^{48, ID},
A.M. Khan ^{120, ID}, S. Khan ^{15, ID}, A. Khanzadeev ^{141, ID}, Y. Kharlov ^{141, ID}, A. Khatun ^{118, ID}, A. Khuntia ^{35, ID},
Z. Khuranova ^{64, ID}, B. Kileng ^{34, ID}, B. Kim ^{104, ID}, C. Kim ^{16, ID}, D.J. Kim ^{117, ID}, E.J. Kim ^{69, ID}, J. Kim ^{139, ID},
J. Kim ^{58, ID}, J. Kim ^{32,69, ID}, M. Kim ^{18, ID}, S. Kim ^{17, ID}, T. Kim ^{139, ID}, K. Kimura ^{92, ID}, A. Kirkova ^{36, ID}, S. Kirsch ^{64, ID},
I. Kisel ^{38, ID}, S. Kiselev ^{141, ID}, A. Kisiel ^{136, ID}, J.P. Kitowski ^{2, ID}, J.L. Klay ^{5, ID}, J. Klein ^{32, ID}, S. Klein ^{74, ID},
C. Klein-Bösing ^{126, ID}, M. Kleiner ^{64, ID}, T. Klemenz ^{95, ID}, A. Kluge ^{32, ID}, C. Kobdaj ^{105, ID}, R. Kohara ^{124, ID},
T. Kollegger ^{97, ID}, A. Kondratyev ^{142, ID}, N. Kondratyeva ^{141, ID}, J. Konig ^{64, ID}, S.A. Konigstorfer ^{95, ID},
P.J. Konopka ^{32, ID}, G. Kornakov ^{136, ID}, M. Korwieser ^{95, ID}, S.D. Koryciak ^{2, ID}, C. Koster ^{84, ID}, A. Kotliarov ^{86, ID},
N. Kovacic ^{89, ID}, V. Kovalenko ^{141, ID}, M. Kowalski ^{107, ID}, V. Kozuharov ^{36, ID}, I. Králik ^{60, ID}, A. Kravčáková ^{37, ID},
L. Krcal ^{32,38, ID}, M. Krivda ^{100,60, ID}, F. Krizek ^{86, ID}, K. Krizkova Gajdosova ^{32, ID}, C. Krug ^{66, ID}, M. Krüger ^{64, ID},
D.M. Krupova ^{35, ID}, E. Kryshen ^{141, ID}, V. Kučera ^{58, ID}, C. Kuhn ^{129, ID}, P.G. Kuijer ^{84, ID}, T. Kumaoka ^{125, ID},
D. Kumar ^{135, ID}, L. Kumar ^{90, ID}, N. Kumar ^{90, ID}, S. Kumar ^{31, ID}, S. Kundu ^{32, ID}, P. Kurashvili ^{79, ID}, A. Kurepin ^{141, ID},
A.B. Kurepin ^{141, ID}, A. Kuryakin ^{141, ID}, S. Kushpil ^{86, ID}, V. Kuskov ^{141, ID}, M. Kutyla ^{136, ID}, A. Kuznetsov ^{142, ID},
M.J. Kweon ^{58, ID}, Y. Kwon ^{139, ID}, S.L. La Pointe ^{38, ID}, P. La Rocca ^{26, ID}, A. Laskrathok ^{105, ID}, M. Lamanna ^{32, ID},
A.R. Landou ^{73, ID}, R. Langoy ^{121, ID}, P. Larionov ^{32, ID}, E. Laudi ^{32, ID}, L. Lautner ^{32,95, ID}, R.A.N. Laveaga ^{109, ID},
R. Lavicka ^{102, ID}, R. Lea ^{134,55, ID}, H. Lee ^{104, ID}, I. Legrand ^{45, ID}, G. Legras ^{126, ID}, J. Lehrbach ^{38, ID}, A.M. Lejeune ^{35, ID},
T.M. Lelek ^{2, ID}, R.C. Lemmon ^{85, ID}, I. León Monzón ^{109, ID}, M.M. Lesch ^{95, ID}, E.D. Lesser ^{18, ID}, P. Lévali ^{46, ID}, M. Li ^{6, ID},
X. Li ^{10, ID}, B.E. Liang-gilman ^{18, ID}, J. Lien ^{121, ID}, R. Lietava ^{100, ID}, I. Likmeta ^{116, ID}, B. Lim ^{24, ID}, S.H. Lim ^{16, ID},
V. Lindenstruth ^{38, ID}, A. Lindner ^{45, ID}, C. Lippmann ^{97, ID}, D.H. Liu ^{6, ID}, J. Liu ^{119, ID}, G.S.S. Liveraro ^{111, ID},
I.M. Lofnes ^{20, ID}, C. Loizides ^{87, ID}, S. Lokos ^{107, ID}, J. Lömkner ^{59, ID}, X. Lopez ^{127, ID}, E. López Torres ^{7, ID},
C. Lotteau ^{128, ID}, P. Lu ^{97,120, ID}, F.V. Lugo ^{67, ID}, J.R. Luhder ^{126, ID}, M. Lunardon ^{27, ID}, G. Luparello ^{57, ID},
Y.G. Ma ^{39, ID}, M. Mager ^{32, ID}, A. Maire ^{129, ID}, E.M. Majerz ^{2, ID}, M.V. Makarieva ^{36, ID}, M. Malaev ^{141, ID},
G. Malfattore ^{25, ID}, N.M. Malik ^{91, ID}, Q.W. Malik ^{19, ID}, S.K. Malik ^{91, ID}, L. Malinina ^{142, ID}, I.VIII, D. Mallick ^{131, ID},
N. Mallick ^{48, ID}, G. Mandaglio ^{30,53, ID}, S.K. Mandal ^{79, ID}, A. Manea ^{63, ID}, V. Manko ^{141, ID}, F. Manso ^{127, ID},
V. Manzari ^{50, ID}, Y. Mao ^{6, ID}, R.W. Marcjan ^{2, ID}, G.V. Margagliotti ^{23, ID}, A. Margotti ^{51, ID}, A. Marín ^{97, ID},
C. Markert ^{108, ID}, P. Martinengo ^{32, ID}, M.I. Martínez ^{44, ID}, G. Martínez García ^{103, ID}, M.P.P. Martins ^{110, ID},
S. Masciocchi ^{97, ID}, M. Masera ^{24, ID}, A. Masoni ^{52, ID}, L. Massacrier ^{131, ID}, O. Massen ^{59, ID}, A. Mastroserio ^{132,50, ID},
O. Matonoha ^{75, ID}, S. Mattiazzo ^{27, ID}, A. Matyja ^{107, ID}, A.L. Mazuecos ^{32, ID}, F. Mazzaschi ^{32,24, ID}, M. Mazzilli ^{116, ID},
J.E. Mdhluli ^{123, ID}, Y. Melikyan ^{43, ID}, M. Melo ^{110, ID}, A. Menchaca-Rocha ^{67, ID}, J.E.M. Mendez ^{65, ID},
E. Meninno ^{102, ID}, A.S. Menon ^{116, ID}, M.W. Menzel ^{32,94, ID}, M. Meres ^{13, ID}, Y. Miake ^{125, ID}, L. Micheletti ^{32, ID},
D.L. Mihaylov ^{95, ID}, K. Mikhaylov ^{142,141, ID}, N. Minafra ^{118, ID}, D. Miśkowiec ^{97, ID}, A. Modak ^{134,4, ID}, B. Mohanty ^{80, ID},
M. Mohisin Khan ^{15, ID}, M.A. Molander ^{43, ID}, S. Monira ^{136, ID}, C. Mordasini ^{117, ID}, D.A. Moreira De Godoy ^{126, ID},
I. Morozov ^{141, ID}, A. Morsch ^{32, ID}, T. Mrnjavac ^{32, ID}, V. Muccifora ^{49, ID}, S. Muhuri ^{135, ID}, J.D. Mulligan ^{74, ID},
A. Mulliri ^{22, ID}, M.G. Munhoz ^{110, ID}, R.H. Munzer ^{64, ID}, H. Murakami ^{124, ID}, S. Murray ^{114, ID}, L. Musa ^{32, ID},
J. Musinsky ^{60, ID}, J.W. Myrcha ^{136, ID}, B. Naik ^{123, ID}, A.I. Nambrath ^{18, ID}, B.K. Nandi ^{47, ID}, R. Nania ^{51, ID},
E. Nappi ^{50, ID}, A.F. Nassirpour ^{17, ID}, A. Nath ^{94, ID}, S. Nath ^{135, ID}, C. Nattrass ^{122, ID}, M.N. Naydenov ^{36, ID},
A. Neagu ^{19, ID}, A. Negru ^{113, ID}, E. Nekrasova ^{141, ID}, L. Nellen ^{65, ID}, R. Nepeivoda ^{75, ID}, S. Nese ^{19, ID}, G. Neskovic ^{38, ID},
N. Nicassio ^{50, ID}, B.S. Nielsen ^{83, ID}, E.G. Nielsen ^{83, ID}, S. Nikolaev ^{141, ID}, S. Nikulin ^{141, ID}, V. Nikulin ^{141, ID},
F. Noferini ^{51, ID}, S. Noh ^{12, ID}, P. Nomokonov ^{142, ID}, J. Norman ^{119, ID}, N. Novitzky ^{87, ID}, P. Nowakowski ^{136, ID},
A. Nyanin ^{141, ID}, J. Nystrand ^{20, ID}, S. Oh ^{17, ID}, A. Ohlson ^{75, ID}, V.A. Okorokov ^{141, ID}, J. Oleniacz ^{136, ID},
A. Onnerstad ^{117, ID}, C. Oppedisano ^{56, ID}, A. Ortiz Velasquez ^{65, ID}, J. Otwinowski ^{107, ID}, M. Oya ^{92, ID}, K. Oyama ^{76, ID},
Y. Pachmayer ^{94, ID}, S. Padhan ^{47, ID}, D. Pagano ^{134,55, ID}, G. Paić ^{65, ID}, S. Paisano-Guzmán ^{44, ID}, A. Palasciano ^{50, ID},

- S. Panebianco 130, ID, C. Pantouvakis 27, ID, H. Park 125, ID, H. Park 104, ID, J. Park 125, ID, J.E. Parkkila 32, ID,
 Y. Patley 47, ID, R.N. Patra 50, B. Paul 135, ID, H. Pei 6, ID, T. Peitzmann 59, ID, X. Peng 11, ID, M. Pennisi 24, ID,
 S. Perciballi 24, ID, D. Peresunko 141, ID, G.M. Perez 7, ID, Y. Pestov 141, M.T. Petersen 83, V. Petrov 141, ID,
 M. Petrovici 45, ID, S. Piano 57, ID, M. Pikna 13, ID, P. Pillot 103, ID, O. Pinazza 51,32, ID, L. Pinsky 116, C. Pinto 95, ID,
 S. Pisano 49, ID, M. Płoskoń 74, ID, M. Planinic 89, F. Pliquet 64, D.K. Plociennik 2, ID, M.G. Poghosyan 87, ID,
 B. Polichtchouk 141, ID, S. Politano 29, ID, N. Poljak 89, ID, A. Pop 45, ID, S. Porteboeuf-Houssais 127, ID,
 V. Pozdniakov 142, ID, I.Y. Pozos 44, ID, K.K. Pradhan 48, ID, S.K. Prasad 4, ID, S. Prasad 48, ID, R. Preghenella 51, ID,
 F. Prino 56, ID, C.A. Pruneau 137, ID, I. Pshenichnov 141, ID, M. Puccio 32, ID, S. Pucillo 24, ID, S. Qiu 84, ID,
 L. Quaglia 24, ID, S. Ragoni 14, ID, A. Rai 138, ID, A. Rakotozafindrabe 130, ID, L. Ramello 133,56, ID, F. Rami 129, ID,
 M. Rasa 26, ID, S.S. Räsänen 43, ID, R. Rath 51, ID, M.P. Rauch 20, ID, I. Ravasenga 32, ID, K.F. Read 87,122, ID,
 C. Reckziegel 112, ID, A.R. Redelbach 38, ID, K. Redlich 79, ID, VII, C.A. Reetz 97, ID, H.D. Regules-Medel 44,
 A. Rehman 20, F. Reidt 32, ID, H.A. Reme-Ness 34, ID, Z. Rescakova 37, K. Reygers 94, ID, A. Riabov 141, ID,
 V. Riabov 141, ID, R. Ricci 28, ID, M. Richter 20, ID, A.A. Riedel 95, ID, W. Riegler 32, ID, A.G. Riffero 24, ID,
 M. Rignanese 27, ID, C. Ripoli 28, C. Ristea 63, ID, M.V. Rodriguez 32, ID, M. Rodríguez Cahuantzi 44, ID,
 S.A. Rodríguez Ramírez 44, ID, K. Røed 19, ID, R. Rogalev 141, ID, E. Rogochaya 142, ID, T.S. Rogoschinski 64, ID,
 D. Rohr 32, ID, D. Röhrich 20, ID, S. Rojas Torres 35, ID, P.S. Rokita 136, ID, G. Romanenko 25, ID, F. Ronchetti 49, ID,
 E.D. Rosas 65, K. Roslon 136, ID, A. Rossi 54, ID, A. Roy 48, ID, S. Roy 47, ID, N. Rubini 51,25, ID, J.A. Rudolph 84,
 D. Ruggiano 136, ID, R. Rui 23, ID, P.G. Russek 2, ID, R. Russo 84, ID, A. Rustamov 81, ID, E. Ryabinkin 141, ID,
 Y. Ryabov 141, ID, A. Rybicki 107, ID, J. Ryu 16, ID, W. Rzesz 136, ID, B. Sabiu 51, S. Sadovsky 141, ID, J. Saetre 20, ID,
 K. Šafařík 35, ID, S.K. Saha 4, ID, S. Saha 80, ID, B. Sahoo 48, ID, R. Sahoo 48, ID, S. Sahoo 61, D. Sahu 48, ID,
 P.K. Sahu 61, ID, J. Saini 135, ID, K. Sajdakova 37, S. Sakai 125, ID, M.P. Salvan 97, ID, S. Sambyal 91, ID, D. Samitz 102, ID,
 I. Sanna 32,95, ID, T.B. Saramela 110, D. Sarkar 83, ID, P. Sarma 41, ID, V. Sarritzu 22, ID, V.M. Sarti 95, ID,
 M.H.P. Sas 32, ID, S. Sawan 80, ID, E. Scapparone 51, ID, J. Schambach 87, ID, H.S. Scheid 64, ID, C. Schiaua 45, ID,
 R. Schicker 94, ID, F. Schlepper 94, ID, A. Schmah 97, C. Schmidt 97, ID, H.R. Schmidt 93, M.O. Schmidt 32, ID,
 M. Schmidt 93, N.V. Schmidt 87, ID, A.R. Schmier 122, ID, R. Schotter 129, ID, A. Schröter 38, ID, J. Schukraft 32, ID,
 K. Schweda 97, ID, G. Scioli 25, ID, E. Scomparin 56, ID, J.E. Seger 14, ID, Y. Sekiguchi 124, D. Sekihata 124, ID,
 M. Selina 84, ID, I. Selyuzhenkov 97, ID, S. Senyukov 129, ID, J.J. Seo 94, ID, D. Serebryakov 141, ID, L. Serkin 65, ID,
 L. Šerkšnytė 95, ID, A. Sevcenco 63, ID, T.J. Shaba 68, ID, A. Shabetai 103, ID, R. Shahoyan 32, A. Shangaraev 141, ID,
 B. Sharma 91, ID, D. Sharma 47, ID, H. Sharma 54, ID, M. Sharma 91, ID, S. Sharma 76, ID, S. Sharma 91, ID,
 U. Sharma 91, ID, A. Shatat 131, ID, O. Sheibani 116, K. Shigaki 92, ID, M. Shimomura 77, J. Shin 12, S. Shirinkin 141, ID,
 Q. Shou 39, ID, Y. Sibiriak 141, ID, S. Siddhanta 52, ID, T. Siemiaczuk 79, ID, T.F. Silva 110, ID, D. Silvermyr 75, ID,
 T. Simantathammakul 105, R. Simeonov 36, ID, B. Singh 91, B. Singh 95, ID, K. Singh 48, ID, R. Singh 80, ID,
 R. Singh 91, ID, R. Singh 97, ID, S. Singh 15, ID, V.K. Singh 135, ID, V. Singhal 135, ID, T. Sinha 99, ID, B. Sitar 13, ID,
 M. Sitta 133,56, ID, T.B. Skaali 19, G. Skorodumovs 94, ID, N. Smirnov 138, ID, R.J.M. Snellings 59, ID, E.H. Solheim 19, ID,
 J. Song 16, ID, C. Sonnabend 32,97, ID, J.M. Sonneveld 84, ID, F. Soramel 27, ID, A.B. Soto-hernandez 88, ID,
 R. Spijkers 84, ID, I. Sputowska 107, ID, J. Staa 75, ID, J. Stachel 94, ID, I. Stan 63, ID, P.J. Steffanic 122, ID,
 S.F. Stiefelmaier 94, ID, D. Stocco 103, ID, I. Storehaug 19, ID, N.J. Strangmann 64, ID, P. Stratmann 126, ID,
 S. Strazzi 25, ID, A. Sturniolo 30,53, ID, C.P. Stylianidis 84, A.A.P. Suaide 110, ID, C. Suire 131, ID, M. Sukhanov 141, ID,
 M. Suljic 32, ID, R. Sultanov 141, ID, V. Sumberia 91, ID, S. Sumowidagdo 82, ID, I. Szarka 13, ID, M. Szymkowski 136, ID,
 S.F. Taghavi 95, ID, G. Taillepied 97, ID, J. Takahashi 111, ID, G.J. Tambave 80, ID, S. Tang 6, ID, Z. Tang 120, ID,
 J.D. Tapia Takaki 118, ID, N. Tapus 113, L.A. Tarasovicova 126, ID, M.G. Tarzila 45, ID, G.F. Tassielli 31, ID,
 A. Tauro 32, ID, A. Tavira García 131, ID, G. Tejeda Muñoz 44, ID, A. Telesca 32, ID, L. Terlizzi 24, ID, C. Terrevoli 50, ID,

- S. Thakur^{4, ID}, D. Thomas^{108, ID}, A. Tikhonov^{141, ID}, N. Tiltmann^{32,126, ID}, A.R. Timmins^{116, ID}, M. Tkacik¹⁰⁶,
 T. Tkacik^{106, ID}, A. Toia^{64, ID}, R. Tokumoto⁹², S. Tomassini²⁵, K. Tomohiro⁹², N. Topilskaya^{141, ID},
 M. Toppi^{49, ID}, V.V. Torres^{103, ID}, A.G. Torres Ramos^{31, ID}, A. Trifiró^{30,53, ID}, T. Triloki⁹⁶, A.S. Triolo^{32,30,53, ID},
 S. Tripathy^{32, ID}, T. Tripathy^{47, ID}, V. Trubnikov^{3, ID}, W.H. Trzaska^{117, ID}, T.P. Trzcinski^{136, ID}, C. Tsolanta¹⁹,
 R. Tu³⁹, A. Tumkin^{141, ID}, R. Turrisi^{54, ID}, T.S. Tveter^{19, ID}, K. Ullaland^{20, ID}, B. Ulukutlu^{95, ID}, A. Uras^{128, ID},
 M. Urioni^{134, ID}, G.L. Usai^{22, ID}, M. Vala³⁷, N. Valle^{55, ID}, L.V.R. van Doremalen⁵⁹, M. van Leeuwen^{84, ID},
 C.A. van Veen^{94, ID}, R.J.G. van Weelden^{84, ID}, P. Vande Vyvre^{32, ID}, D. Varga^{46, ID}, Z. Varga^{46, ID},
 P. Vargas Torres⁶⁵, M. Vasileiou^{78, ID}, A. Vasiliev^{141, ID}, O. Vázquez Doce^{49, ID}, O. Vazquez Rueda^{116, ID},
 V. Vechernin^{141, ID}, E. Vercellin^{24, ID}, S. Vergara Limón⁴⁴, R. Verma⁴⁷, L. Vermunt^{97, ID}, R. Vértesi^{46, ID},
 M. Verweij^{59, ID}, L. Vickovic³³, Z. Vilakazi¹²³, O. Villalobos Baillie^{100, ID}, A. Villani^{23, ID}, A. Vinogradov^{141, ID},
 T. Virgili^{28, ID}, M.M.O. Virta^{117, ID}, A. Vodopyanov^{142, ID}, B. Volkel^{32, ID}, M.A. Völkl^{94, ID}, S.A. Voloshin^{137, ID},
 G. Volpe^{31, ID}, B. von Haller^{32, ID}, I. Vorobyev^{32, ID}, N. Vozniuk^{141, ID}, J. Vrláková^{37, ID}, J. Wan³⁹, C. Wang^{39, ID},
 D. Wang³⁹, Y. Wang^{39, ID}, Y. Wang^{6, ID}, A. Wegrzynek^{32, ID}, F.T. Weiglhofer³⁸, S.C. Wenzel^{32, ID},
 J.P. Wessels^{126, ID}, J. Wiechula^{64, ID}, J. Wikne^{19, ID}, G. Wilk^{79, ID}, J. Wilkinson^{97, ID}, G.A. Willems^{126, ID},
 B. Windelband^{94, ID}, M. Winn^{130, ID}, J.R. Wright^{108, ID}, W. Wu³⁹, Y. Wu^{120, ID}, Z. Xiong¹²⁰, R. Xu^{6, ID},
 A. Yadav^{42, ID}, A.K. Yadav^{135, ID}, Y. Yamaguchi^{92, ID}, S. Yang²⁰, S. Yano^{92, ID}, E.R. Yeats¹⁸, Z. Yin^{6, ID},
 I.-K. Yoo^{16, ID}, J.H. Yoon^{58, ID}, H. Yu¹², S. Yuan²⁰, A. Yuncu^{94, ID}, V. Zaccolo^{23, ID}, C. Zampolli^{32, ID},
 F. Zanone^{94, ID}, N. Zardoshti^{32, ID}, A. Zarochentsev^{141, ID}, P. Závada^{62, ID}, N. Zaviyalov¹⁴¹, M. Zhalov^{141, ID},
 B. Zhang^{6, ID}, C. Zhang^{130, ID}, L. Zhang^{39, ID}, M. Zhang^{127,6, ID}, M. Zhang^{6, ID}, S. Zhang^{39, ID}, X. Zhang^{6, ID},
 Y. Zhang¹²⁰, Z. Zhang^{6, ID}, M. Zhao^{10, ID}, V. Zherebchevskii^{141, ID}, Y. Zhi¹⁰, D. Zhou^{6, ID}, Y. Zhou^{83, ID},
 J. Zhu^{54,6, ID}, S. Zhu¹²⁰, Y. Zhu⁶, S.C. Zugravel^{56, ID}, N. Zurlo^{134,55, ID}

¹ A.I. Alikhanyan National Science Laboratory (Yerevan Physics Institute) Foundation, Yerevan, Armenia² AGH University of Krakow, Cracow, Poland³ Bogolyubov Institute for Theoretical Physics, National Academy of Sciences of Ukraine, Kiev, Ukraine⁴ Bose Institute, Department of Physics and Centre for Astroparticle Physics and Space Science (CAPSS), Kolkata, India⁵ California Polytechnic State University, San Luis Obispo, CA, United States⁶ Central China Normal University, Wuhan, China⁷ Centro de Aplicaciones Tecnológicas y Desarrollo Nuclear (CEADEN), Havana, Cuba⁸ Centro de Investigación y de Estudios Avanzados (CINVESTAV), Mexico City and Mérida, Mexico⁹ Chicago State University, Chicago, IL, United States¹⁰ China Institute of Atomic Energy, Beijing, China¹¹ China University of Geosciences, Wuhan, China¹² Chungbuk National University, Cheongju, Republic of Korea¹³ Comenius University Bratislava, Faculty of Mathematics, Physics and Informatics, Bratislava, Slovak Republic¹⁴ Creighton University, Omaha, NE, United States¹⁵ Department of Physics, Aligarh Muslim University, Aligarh, India¹⁶ Department of Physics, Pusan National University, Pusan, Republic of Korea¹⁷ Department of Physics, Sejong University, Seoul, Republic of Korea¹⁸ Department of Physics, University of California, Berkeley, CA, United States¹⁹ Department of Physics, University of Oslo, Oslo, Norway²⁰ Department of Physics and Technology, University of Bergen, Bergen, Norway²¹ Dipartimento di Fisica, Università di Pavia, Pavia, Italy²² Dipartimento di Fisica dell'Università e Sezione INFN, Cagliari, Italy²³ Dipartimento di Fisica dell'Università e Sezione INFN, Trieste, Italy²⁴ Dipartimento di Fisica dell'Università e Sezione INFN, Turin, Italy²⁵ Dipartimento di Fisica e Astronomia dell'Università e Sezione INFN, Bologna, Italy²⁶ Dipartimento di Fisica e Astronomia dell'Università e Sezione INFN, Catania, Italy²⁷ Dipartimento di Fisica e Astronomia dell'Università e Sezione INFN, Padova, Italy²⁸ Dipartimento di Fisica 'E.R. Caianiello' dell'Università e Gruppo Collegato INFN, Salerno, Italy²⁹ Dipartimento DISAT del Politecnico and Sezione INFN, Turin, Italy³⁰ Dipartimento di Scienze MIFT, Università di Messina, Messina, Italy³¹ Dipartimento Interateneo di Fisica 'M. Merlin' and Sezione INFN, Bari, Italy³² European Organization for Nuclear Research (CERN), Geneva, Switzerland³³ Faculty of Electrical Engineering, Mechanical Engineering and Naval Architecture, University of Split, Split, Croatia³⁴ Faculty of Engineering and Science, Western Norway University of Applied Sciences, Bergen, Norway³⁵ Faculty of Nuclear Sciences and Physical Engineering, Czech Technical University in Prague, Prague, Czech Republic³⁶ Faculty of Physics, Sofia University, Sofia, Bulgaria³⁷ Faculty of Science, P.J. Šafárik University, Košice, Slovak Republic³⁸ Frankfurt Institute for Advanced Studies, Johann Wolfgang Goethe-Universität Frankfurt, Frankfurt, Germany³⁹ Fudan University, Shanghai, China⁴⁰ Gangneung-Wonju National University, Gangneung, Republic of Korea

- ⁴¹ Gauhati University, Department of Physics, Guwahati, India
⁴² Helmholtz-Institut für Strahlen- und Kernphysik, Rheinische Friedrich-Wilhelms-Universität Bonn, Bonn, Germany
⁴³ Helsinki Institute of Physics (HIP), Helsinki, Finland
⁴⁴ High Energy Physics Group, Universidad Autónoma de Puebla, Puebla, Mexico
⁴⁵ Horia Hulubei National Institute of Physics and Nuclear Engineering, Bucharest, Romania
⁴⁶ HUN-REN Wigner Research Centre for Physics, Budapest, Hungary
⁴⁷ Indian Institute of Technology Bombay (IIT), Mumbai, India
⁴⁸ Indian Institute of Technology Indore, Indore, India
⁴⁹ INFN, Laboratori Nazionali di Frascati, Frascati, Italy
⁵⁰ INFN, Sezione di Bari, Bari, Italy
⁵¹ INFN, Sezione di Bologna, Bologna, Italy
⁵² INFN, Sezione di Cagliari, Cagliari, Italy
⁵³ INFN, Sezione di Catania, Catania, Italy
⁵⁴ INFN, Sezione di Padova, Padova, Italy
⁵⁵ INFN, Sezione di Pavia, Pavia, Italy
⁵⁶ INFN, Sezione di Torino, Turin, Italy
⁵⁷ INFN, Sezione di Trieste, Trieste, Italy
⁵⁸ Inha University, Incheon, Republic of Korea
⁵⁹ Institute for Gravitational and Subatomic Physics (GRASP), Utrecht University/Nikhef, Utrecht, Netherlands
⁶⁰ Institute of Experimental Physics, Slovak Academy of Sciences, Košice, Slovak Republic
⁶¹ Institute of Physics, Homi Bhabha National Institute, Bhubaneswar, India
⁶² Institute of Physics of the Czech Academy of Sciences, Prague, Czech Republic
⁶³ Institute of Space Science (ISS), Bucharest, Romania
⁶⁴ Institut für Kernphysik, Johann Wolfgang Goethe-Universität Frankfurt, Frankfurt, Germany
⁶⁵ Instituto de Ciencias Nucleares, Universidad Nacional Autónoma de México, Mexico City, Mexico
⁶⁶ Instituto de Física, Universidade Federal do Rio Grande do Sul (UFRGS), Porto Alegre, Brazil
⁶⁷ Instituto de Física, Universidad Nacional Autónoma de México, Mexico City, Mexico
⁶⁸ iThemba LABS, National Research Foundation, Somerset West, South Africa
⁶⁹ Jeonbuk National University, Jeonju, Republic of Korea
⁷⁰ Johann-Wolfgang-Goethe Universität Frankfurt Institut für Informatik, Fachbereich Informatik und Mathematik, Frankfurt, Germany
⁷¹ Korea Institute of Science and Technology Information, Daejeon, Republic of Korea
⁷² KTO Karatay University, Konya, Turkey
⁷³ Laboratoire de Physique Subatomique et de Cosmologie, Université Grenoble-Alpes, CNRS-IN2P3, Grenoble, France
⁷⁴ Lawrence Berkeley National Laboratory, Berkeley, CA, United States
⁷⁵ Lund University Department of Physics, Division of Particle Physics, Lund, Sweden
⁷⁶ Nagasaki Institute of Applied Science, Nagasaki, Japan
⁷⁷ Nara Women's University (NWU), Nara, Japan
⁷⁸ National and Kapodistrian University of Athens, School of Science, Department of Physics, Athens, Greece
⁷⁹ National Centre for Nuclear Research, Warsaw, Poland
⁸⁰ National Institute of Science Education and Research, Homi Bhabha National Institute, Jatni, India
⁸¹ National Nuclear Research Center, Baku, Azerbaijan
⁸² National Research and Innovation Agency - BRIN, Jakarta, Indonesia
⁸³ Niels Bohr Institute, University of Copenhagen, Copenhagen, Denmark
⁸⁴ Nikhef, National institute for subatomic physics, Amsterdam, Netherlands
⁸⁵ Nuclear Physics Group, STFC Daresbury Laboratory, Daresbury, United Kingdom
⁸⁶ Nuclear Physics Institute of the Czech Academy of Sciences, Hlubice-Řež, Czech Republic
⁸⁷ Oak Ridge National Laboratory, Oak Ridge, TN, United States
⁸⁸ Ohio State University, Columbus, OH, United States
⁸⁹ Physics department, Faculty of science, University of Zagreb, Zagreb, Croatia
⁹⁰ Physics Department, Panjab University, Chandigarh, India
⁹¹ Physics Department, University of Jammu, Jammu, India
⁹² Physics Program and International Institute for Sustainability with Knotted Chiral Meta Matter (SKCM2), Hiroshima University, Hiroshima, Japan
⁹³ Physikalisches Institut, Eberhard-Karls-Universität Tübingen, Tübingen, Germany
⁹⁴ Physikalisches Institut, Ruprecht-Karls-Universität Heidelberg, Heidelberg, Germany
⁹⁵ Physik Department, Technische Universität München, Munich, Germany
⁹⁶ Politecnico di Bari and Sezione INFN, Bari, Italy
⁹⁷ Research Division and ExtreMe Matter Institute EMMI, GSI Helmholtzzentrum für Schwerionenforschung GmbH, Darmstadt, Germany
⁹⁸ Saga University, Saga, Japan
⁹⁹ Saha Institute of Nuclear Physics, Homi Bhabha National Institute, Kolkata, India
¹⁰⁰ School of Physics and Astronomy, University of Birmingham, Birmingham, United Kingdom
¹⁰¹ Sección Física, Departamento de Ciencias, Pontificia Universidad Católica del Perú, Lima, Peru
¹⁰² Stefan Meyer Institut für Subatomare Physik (SMI), Vienna, Austria
¹⁰³ SUBATECH, IMT Atlantique, Nantes Université, CNRS-IN2P3, Nantes, France
¹⁰⁴ Sungkyunkwan University, Suwon City, Republic of Korea
¹⁰⁵ Suranaree University of Technology, Nakhon Ratchasima, Thailand
¹⁰⁶ Technical University of Košice, Košice, Slovak Republic
¹⁰⁷ The Henryk Niewodniczanski Institute of Nuclear Physics, Polish Academy of Sciences, Cracow, Poland
¹⁰⁸ The University of Texas at Austin, Austin, TX, United States
¹⁰⁹ Universidad Autónoma de Sinaloa, Culiacán, Mexico
¹¹⁰ Universidade de São Paulo (USP), São Paulo, Brazil
¹¹¹ Universidade Estadual de Campinas (UNICAMP), Campinas, Brazil
¹¹² Universidade Federal do ABC, Santo André, Brazil
¹¹³ Universitatea Națională de Știință și Tehnologie Politehnica Bucuresti, Bucharest, Romania
¹¹⁴ University of Cape Town, Cape Town, South Africa
¹¹⁵ University of Derby, Derby, United Kingdom
¹¹⁶ University of Houston, Houston, TX, United States
¹¹⁷ University of Jyväskylä, Jyväskylä, Finland
¹¹⁸ University of Kansas, Lawrence, KS, United States
¹¹⁹ University of Liverpool, Liverpool, United Kingdom
¹²⁰ University of Science and Technology of China, Hefei, China

- 121 University of South-Eastern Norway, Kongsberg, Norway
122 University of Tennessee, Knoxville, TN, United States
123 University of the Witwatersrand, Johannesburg, South Africa
124 University of Tokyo, Tokyo, Japan
125 University of Tsukuba, Tsukuba, Japan
126 Universität Münster, Institut für Kernphysik, Münster, Germany
127 Université Clermont Auvergne, CNRS/IN2P3, LPC, Clermont-Ferrand, France
128 Université de Lyon, CNRS/IN2P3, Institut de Physique des 2 Infinis de Lyon, Lyon, France
129 Université de Strasbourg, CNRS, IPHC UMR 7178, F-67000 Strasbourg, France, Strasbourg, France
130 Université Paris-Saclay, Centre d'Etudes de Saclay (CEA), IRFU, Département de Physique Nucléaire (DPhN), Saclay, France
131 Université Paris-Saclay, CNRS/IN2P3, IJCLab, Orsay, France
132 Università degli Studi di Foggia, Foggia, Italy
133 Università del Piemonte Orientale, Vercelli, Italy
134 Università di Brescia, Brescia, Italy
135 Variable Energy Cyclotron Centre, Homi Bhabha National Institute, Kolkata, India
136 Warsaw University of Technology, Warsaw, Poland
137 Wayne State University, Detroit, MI, United States
138 Yale University, New Haven, CT, United States
139 Yonsei University, Seoul, Republic of Korea
140 Zentrum für Technologie und Transfer (ZTT), Worms, Germany
141 Affiliated with an institute covered by a cooperation agreement with CERN
142 Affiliated with an international laboratory covered by a cooperation agreement with CERN

^I Deceased.

^{II} Also at: Max-Planck-Institut für Physik, Munich, Germany.

^{III} Also at: Italian National Agency for New Technologies, Energy and Sustainable Economic Development (ENEA), Bologna, Italy.

^{IV} Also at: Dipartimento DET del Politecnico di Torino, Turin, Italy.

^V Also at: Yıldız Technical University, Istanbul, Türkiye.

^{VI} Also at: Department of Applied Physics, Aligarh Muslim University, Aligarh, India.

^{VII} Also at: Institute of Theoretical Physics, University of Wroclaw, Poland.

^{VIII} Also at: An institution covered by a cooperation agreement with CERN.